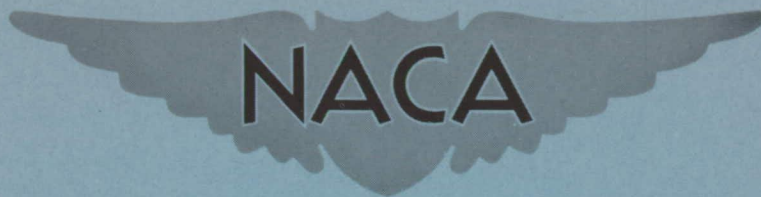RM E53D23   *Superseded by NACA TR-1215*   RM E53D23

NACA

RESEARCH MEMORANDUM

PROCEDURE FOR MEASURING LIQUID-WATER CONTENT AND

DROPLET SIZES IN SUPERCOOLED CLOUDS BY ROTATING

MULTICYLINDER METHOD

By William Lewis, Porter J. Perkins, and
Rinaldo J. Brun

Lewis Flight Propulsion Laboratory
Cleveland, Ohio

NATIONAL ADVISORY COMMITTEE
FOR AERONAUTICS
WASHINGTON
June 29, 1953

NATIONAL ADVISORY COMMITTEE FOR AERONAUTICS

RESEARCH MEMORANDUM

PROCEDURE FOR MEASURING LIQUID-WATER CONTENT AND DROPLET SIZES IN

SUPERCOOLED CLOUDS BY ROTATING MULTICYLINDER METHOD

By William Lewis, Porter J. Perkins, and Rinaldo J. Brun

SUMMARY

The rotating multicylinder method for in-flight determination of
liquid-water content, droplet size, and droplet-size distribution in
icing clouds is described. The theory of operation, the apparatus
required, the technique of obtaining data in flight, and detailed meth-
ods of calculating the results, including necessary charts and tables,
are presented.

INTRODUCTION

A knowledge of the constitution of supercooled clouds is necessary
in order to design equipment for the protection of aircraft components
against ice formation. A commonly used technique for measuring cloud
liquid-water content, droplet size, and droplet-size distribution
involves the collection of ice on cylinders exposed to the air stream
in the icing clouds. This technique is known as the rotating multi-
cylinder method (refs. 1 to 4). In this method, several cylinders of
different diameters rotating on a common axis are exposed from an air-
plane in flight to the supercooled droplets in a cloud. A set of cyl-
inders extended through the fuselage of an airplane is shown in figure 1.

In the usual procedure for obtaining cloud-droplet data, the multi-
cylinders are extended through the airplane fuselage during the exposure
period and are then retracted for disassembling and weighing. It is
assumed that during the exposure period in flight all the supercooled
droplets that strike the cylinders freeze completely on the cylinders.
The cylinders are rotated during exposure in order to secure uniform
ice collection around the circumference, thus preserving a circular
cross section during the entire exposure.

The measurement of droplet size, droplet-size distribution, and
liquid-water content is based on the principle that cylinders of dif-
ferent sizes collect different quantities of ice per unit frontal area.
The amount of ice collected per unit frontal area is expressed in terms

of the collection efficiency, that is, the ratio of the mass of ice collected to the mass of liquid water contained in the volume of space swept by the cylinder. The collection efficiency, which has been determined theoretically (ref. 3), is a known function of droplet size, cylinder size, air speed, air density, and air viscosity. The liquid-water content and the average droplet diameter are determined from a comparison of the measured weight of ice collected on each cylinder with the calculated values of collection efficiency. The actual distribution of cloud-droplet sizes cannot be determined as such by the multicylinder method, but the degree of inhomogeneity can be approximated by comparing the flight data with values of collection efficiency calculated for hypothetical droplet-size distributions. However, indications of droplet-size distribution thus obtained are usually unreliable because of the insensitivity of the method (ref. 3).

The procedure presented herein for determining droplet size, droplet-size distribution, and liquid-water content in clouds is a description of techniques developed by the NACA and others interested in the problem of measuring the characteristics of icing clouds. These techniques are based on the methods originally proposed in reference 1. A description of the apparatus adopted for flight use at the NACA Lewis laboratory, the procedure used in taking data in flight, and the customary method of processing the flight data to determine liquid-water content, average droplet size, and droplet-size distribution constitute the main subject of this report. A brief discussion of the basic theory of the calculations is contained in appendix B, and an alternate method which has recently been devised for processing the flight data is described in appendix C.

The basic steps involved in the application of the multicylinder method are essentially as follows:

(1) Exposure of a set of cylinders of different sizes in the super-cooled cloud for a measured time at a known pressure-altitude, true air speed, and ambient temperature

(2) Disassembly of the cylinders and storage of the ice-covered cylinders in separate water-proof containers

(3) Weighing of the individual cylinders plus containers in both the wet and dry condition to obtain the net weight of collected ice

(4) Determination of liquid-water content, droplet size, and droplet-size distribution by comparing the measured weight of ice collected on eacn cylinder with theoretical computations for comparable cylinders and comparable flight and atmos- pheric conditions

These basic steps are discussed in detail in subsequent sections.

APPARATUS

The following pieces of equipment are used for taking multicylinder data during flight:

(a) Cylinder sets

(b) Shafts and transition segments

(c) Plastic bags (large and small) with rubber bands for sealing

(d) Carrying case for cylinder sets, shafts, and transition segments

(e) Cold box for storage and disassembly of iced cylinders

(f) Box with compartments (not refrigerated) for storing cylinders in sealed bags after disassembly

(g) Rotating drive unit and mast mounted on sliding platform supported by guide rails

(h) Stop watch

(i) Free-air temperature indicator, altimeter, and air-speed indicator

Auxiliary items necessary for use on the ground after the flight are:

(j) Set of balances (accuracy, ±0.01 g)

(k) Drying rack for plastic bags

The essential components of this equipment, including a set of balances, an assembled multicylinder unit, and the carrying case for cylinder sets, are shown in figure 2. The details of an assembled set of cylinders are shown in figure 3. The standard set of cylinders includes 1/8-inch-, 1/2-inch-, $1\frac{1}{4}$-inch-, 3-inch-, and $4\frac{1}{2}$-inch-diameter cylinders which are each 2 inches long. The set is arranged with flanges attached to the ends of the cylinder elements in order to establish precisely the length of the ice samples and to provide for ease in disassembly after exposure to an icing cloud. The transition pieces are designed for minimum distortion of the air-flow field from the required two-dimensional flow pattern around the cylinders.

An assembled set of cylinders is shown in figure 4 in the retracted position. A sliding platform supports the cylinder assembly on a 2-foot mast and a rotating drive unit (not shown in fig. 4) in such a manner

that the entire assembly can be moved to a position in which the mast will be extended into the ambient air stream a sufficient distance to be reasonably free from aerodynamic effects introduced by the fuselage. The details of construction of the sliding platform, the guide rails, and the supporting structure vary depending on the type of airplane and their location in the airplane. The drive unit rotates the supporting mast and multicylinder assembly at a speed of about 80 rpm (speed not critical ±20 rpm).

The wooden cold box used for disassembling should be large enough to hold one or more assembled sets of multicylinders. If time does not permit the immediate disassembling of the cylinders following an exposure, the cold box can be used as a storage box for short durations. Disassembly of the cylinders is facilitated with the cylinders in the vertical position; therefore the box should be so constructed that one side and the top can be opened. The other three sides of the box should be surrounded with dry ice. Sockets should be provided in the bottom of the box for insertion of the driving shaft, which acts as a support for the cylinders.

The ambient air temperature may be measured by any convenient type of thermometer, but the temperature element must be shielded from direct water impingement in order to prevent heat-of-fusion effects. The air speed used in the calculations is the speed of the air with respect to the airplane at the point in the field of flow about the fuselage at which the cylinders are to be exposed. The relation between the true air speed of the airplane, obtained with the air-speed indicator that is part of the original equipment on the airplane, and the required local air speed may be determined experimentally for any particular installation by means of a static-pressure survey. If an appreciable variation (approx. 2 percent) of local air speed exists along a line with the same length and direction as the cylinder assembly, another exposure location on the airplane must be selected. Effects caused by propellers and protruding objects can be evaluated with a static-pressure survey.

OPERATING PROCEDURE

The following procedure and precautions are suggested to insure sufficient and reliable data:

(1) Three sets of cylinders should be assembled prior to flight or before entry into suspected icing conditions.

(2) All unmounted cylinders should be in the carrying rack within convenient reach of the operators.

(3) Plastic bags should be marked according to run number prior to take-off.

(4) When test conditions are established, a set of cylinders should be exposed to the air stream for a period of 1 to 5 minutes, depending upon the rate of ice formation. The ice thickness should always be less than the width of the flanges on the 1/8-inch-diameter cylinder. The period of exposure should be measured to the nearest second and recorded. In order to minimize the errors associated with large percentage changes in cylinder radius, the exposure period should be just long enough to obtain ice samples which can be weighed to an accuracy of 2 percent. The air speed should be held as nearly constant as possible during exposure.

(5) The time involved in extending or retracting the cylinders should be as short as possible in order to minimize the difference in exposure time between the large and the small cylinder.

(6) The complete assembly should be placed in the cold box during the disassembling period.

(7) In the disassembling procedure, the ice should be carefully scraped off the thin flanges at the ends of the cylinders in order to insure that only ice collected on the cylinders will be weighed. If a small amount of ice is lost from a cylinder, the percentage of loss should be estimated and recorded. (A pair of pliers may be necessary occasionally in order to loosen some of the transition segments frozen on the cylinders or shafts. Drying each part with a cloth before reassembling will help to prevent adherence between the parts after exposure.)

(8) The plastic bags in which the ice-coated cylinders are placed should be sealed with rubber bands and deflated to prevent bursting with increase in altitude.

(9) The ice-coated cylinders should be arranged in systematic order in the storage box. The sealed bags should be handled carefully to prevent breakage of bags and possible damage to the cylinders.

(10) Pressure-altitude, free-air temperature, and indicated air speed, averaged over the exposure period, should be taken during exposure. The air speed should be determined as accurately as practicable; approximate values of pressure-altitude and temperature are satisfactory.

(11) After the flight, each cylinder and its plastic bag should be weighed together to the nearest one-hundredth of a gram. After the initial weighing, drying of the bags will be expedited if they are turned inside out. Care should be exercised in making certain that each cylinder is weighed dry with the same rubber band and bag used in the initial weighing.

CALCULATING PROCEDURE

Computed values of collection efficiency presented in reference 3, ice-collection data obtained with the rotating cylinders, and flight data expressed in terms of working parameters are used to determine cloud liquid-water content and droplet size. The working parameters are φ/LU, which involves the factors of pressure-altitude and air temperature, and I, amount of ice collected per unit frontal area. (All symbols are defined in appendix A.)

It is convenient to record the flight data and the computation steps in a systematic form such as the work sheet shown in table I. In the detailed calculation procedure that follows, reference is made to the various numbered items listed in table I.

Before proceeding with the calculations, the flight data are recorded as items (1), (4), (5), and (8). The weight of ice on each cylinder is entered as item (12). Corrections for any loss of ice are made and the corrected weights are entered as item (13).

The calculation procedure is as follows:

Step (a): Calculation of average local air speed. - The average true air speed (item (2)) is obtained by correcting, in the usual manner, the average indicated air speed (item (1)) for air-density effects. The average local air speed to be entered in item (3) is the true air speed corrected (if required) for effects caused by the fuselage of the airplane. This correction factor is obtained by the static-pressure survey mentioned in the preceding section on apparatus.

Step (b): Calculation of free-air temperature. - The wet-air-temperature correction (item (6)) is obtained from the relation (ref. 5)

$$\Delta T = - rV^2 \frac{\alpha_s}{\alpha_d} \times 10^{-4}$$

Although the recovery factor is influenced to a slight extent by several factors, including shape, thermal conductivity, and location of the temperature probe, a value of 0.85 for r is suggested unless a calibration of the installation is available. The lapse-rate ratio α_s/α_d is given in figure 5 as a function of the pressure-altitude and temperature (items (4) and (5)). As will be observed when use is made of the corrected temperature (item (7)), which is the algebraic sum of items (5) and (6), small inaccuracies in the temperature ($\pm 2^\circ$ C) will not appreciably affect the final results.

Step (c): Calculation of φ/LU parameter. - The φ/LU parameter has been found a convenient means of introducing the effects of altitude and temperature into the calculations required for the determination of droplet size and droplet-size distribution. The value of φ/LU (item (9)) is obtained from figure 6, in which the corrected temperature (item (7)) is used.

Step (d): Calculation of average cylinder radius. - The values of L (item (14)) are calculated by using the equation

$$L = \frac{1}{2}\left(L_0 + \sqrt{\frac{m}{\rho_i \pi l} + L_0^2}\right)$$

The recommended average value of the ice density ρ_i is 0.85 gram per cubic centimeter and, for the apparatus described herein, $l = 5.08$ centimeters; hence the equation becomes

$$L = \frac{1}{2}\left(L_0 + \sqrt{0.0737m + L_0^2}\right)$$

Note. - Experience on Mt. Washington has shown that more reliable results may be obtained from actual measurement of the final diameter (ref. 4); however, this procedure is usually not practicable in flight. Moreover, the density of ice collected in flight is higher and more uniform than that of ice collected on Mt. Washington because of the higher air speed in flight. For flight data, therefore, measurement of the final diameter is not considered advantageous in view of the practical difficulties involved.

Step (e): Calculation of relative amount of ice per unit frontal area. - The mass of ice collected per unit frontal area is determined by the following equation:

$$I = 1.118 \times 10^4 \frac{m}{Ll}$$

For the cylinders shown in figure 3, the length of the cylinders l is 5.08 centimeters and the equation becomes

$$I = 2.20 \times 10^3 \frac{m}{L}$$

Values of I for each cylinder are entered as item (15).

Step (f): Plotting. - A plot of I as a function of L is constructed on logarithmic graph paper. A sample plot is shown in figure 7. The plotted points are not connected because the subsequent step involves matching the plotted points to a curve.

Step (g): Matching procedure. - The liquid-water content, droplet size, and droplet-size distribution in the cloud are found by comparing the measured values of I, plotted as indicated in step (f), with calculated values for the cylinders in the same flight and atmospheric conditions. The theoretical values are available in terms of several convenient dimensionless parameters that are explained in appendix B. For matching with the flight data, sets of curves are required that represent the relation between the reciprocal of the inertia parameter $1/K_0$ and the over-all weighted collection efficiency E_ω for five assumed droplet-size distributions for each of four arbitrarily selected values of $K_0 \varphi$ (200, 1000, 3000, or 10,000) that are hereinafter called standard values. These curves (sample shown in fig. 8) are prepared by plotting the data of table II on logarithmic graph paper of the same scale as that used for plotting the measured data (step(f)). Values of E_ω for distributions A, B, C, D, and E, defined in table III, have been multiplied by the constant factors 0.6, 0.7, 0.8, 0.9, and 1.0, respectively, in order that the values may be plotted as five curves for one value of $K_0 \varphi$ on a single sheet of 2-by-3-cycle logarithmic graph paper without overlapping (fig. 8). Use of the curves is facilitated if the location of the line for which $1/K_0 = 1$ and each of the lines for which $E_\omega = 1$ (corresponding to the five size distributions) are clearly marked.

The matching of the measured data with the theoretical calculations usually requires several steps of successive approximations in order to satisfy several restrictive conditions simultaneously. The principle underlying the stepwise procedure is discussed briefly in appendix B. The stepwise procedure for matching the curves is as follows:

(1) A preliminary estimate of a value of $K_0 \varphi$ from the standard values of $K_0 \varphi$ given in table II is used for item (16-A). A value of 3000 is suggested unless experience dictates that other values are closer approximations. An incorrect preliminary estimate will not lead to an incorrect final result but will perhaps require extra successive approximations.

(2) The set of theoretical curves of E_ω as a function of $1/K_0$ applicable to the selected standard value of $K_0 \varphi$ (item (16-A)) is compared with the experimental plot prepared in step (f). The experimental plot is placed over the theoretical curves and viewed by transmitted light. The sheet containing the experimental points is moved

about, with the two sets of axes kept parallel, until the position of best fit is obtained. The principle which underlies this step in matching is discussed in appendix B. The various curves for different droplet-size distributions are tried, and the one that most closely fits the experimental points is selected. The letter designating the curve of best fit is recorded as the droplet-size distribution, item (20-B). While the two plots are held in the position of best fit, the value of L that falls upon the line for which $1/K_O = 1$ and the value of I that falls along the line for which $E_\omega = 1$ are recorded as LK_O (item (17-B)) and Utw (item (21-B)), respectively.

(3) A corrected value of $K_O\phi$ (item (18-B)) is obtained by multiplying the value of LK_O in item (17-B) by ϕ/LU (item (9)) and U (item (3)). The standard value of $K_O\phi$ corresponding to item (18-B) is selected from the following table and entered as item (16-B):

Range of estimated or calculated $K_O\phi$	Corresponding standard value of $K_O\phi$
200 to 440	200
441 to 1,750	1,000
1,751 to 5,600	3,000
5,601 to 30,000	10,000

If item (16-B) is the same as item (16-A), items (17-B) and (21-B) are used in step (h). If item (16-B) is different from item (16-A), the procedure of the second paragraph of step (g) is repeated, and the curves applicable to the new standard value of $K_O\phi$ (item (16-B)) are used.

Step (h): Calculation of droplet diameter and liquid-water content. - The end results of step (g) are values of Utw (item (21-C) or (21-B)), LK_O (item (17-C) or (17-B)), droplet-size distribution (item (20-C) or (20-B)), and $K_O\phi$ (item (18-C) or (18-B)), all of which were obtained with the curves based on the standard value of $K_O\phi$ that corresponds to the actual value of $K_O\phi$. These results are used to determine the droplet diameter and the liquid-water content as follows:

(1) The uncorrected droplet diameter (item (19-C)) is obtained from figure 9 by using items (17), (3), and (7).

(2) The droplet-diameter correction factor (item (22)), obtained from figure 10 by using items (18) and (16), is multiplied by item (19-C) to obtain the final value of droplet diameter d (item (23)). The droplet diameter obtained by this procedure is often referred to as the "mean-effective droplet diameter."

(3) The liquid-water content w (item (24)) is obtained by dividing item (21) by Ut (item (3) multiplied by item (8)).

CONCLUDING REMARKS

The rotating multicylinder method for determining cloud-droplet size and liquid-water content has several inherent disadvantages; however, it is considered to be the most reliable technique known at this time that is adaptable to flight use. The meteorological data obtained with the multicylinder method are the only data available for the design of ice-protection equipment for aircraft. An important disadvantage of the method lies in its insensitivity in discriminating among different droplet-size distributions. An evaluation of the sensitivity is presented in reference 3. Another disadvantage is that the droplet-size distribution obtained by the multicylinder method is not necessarily the actual droplet-size distribution existing in the cloud but rather an assumed droplet-size distribution (table III). Although the actual droplet-size distribution in the cloud may affect the amount of ice collected on the cylinders in the manner described by the theoretical computations for an assumed droplet-size distribution, the area of coverage on an airfoil, or on other nonrotating members, in the cloud may differ from the area theoretically computed on the basis of the assumed distribution indicated by the rotating multicylinder method. The reason for the difference in area, or extent of coverage, is that the size of the largest droplets in the assumed distribution (given as a ratio to the volume median) is an arbitrarily assumed value, and the multicylinder method does not provide a means for obtaining this value from the cloud data.

In obtaining the flight data, the airplane speed should be maintained as low as possible, because the final results are most accurate with low speeds. A discussion of the possible errors as a function of airplane speed and other variables is presented in reference 3. The limitations of the ice accretion rate caused by kinetic heating and heat of fusion are less severe at low air speeds (ref. 6).

A discussion of different forms of the multicylinder instruments and the effects of yaw, ice density, and other factors on the reliability of data and the reproducibility of measurements for conditions on a mountain is contained in reference 4.

Lewis Flight Propulsion Laboratory
      National Advisory Committee for Aeronautics
            Cleveland, Ohio, February 6, 1953

APPENDIX A

SYMBOLS

The following symbols and units are used in this report:

a   radius of cloud droplet, cm

c   constant

d   mean-effective diameter of cloud droplet, microns $(d = 2 \times 10^4 a)$

E   collection efficiency, dimensionless

I   amount of ice collected per unit frontal area of cylinder, (miles/hr)(sec)(g/cu m)

I'   amount of ice collected per unit frontal area of cylinder, g/sq cm

K   inertia parameter, $2\rho_w a^2 U'/9\mu L$, dimensionless

L   average radius of ice-covered cylinder, cm

L_0 radius of ice-free cylinder, cm

l length of cylinder, cm

m   mass of ice collected on cylinder, g

r   temperature recovery factor, dimensionless

T   free-air temperature (corrected for wet-air kinetic heating), $^{\circ}C$

ΔT wet-air kinetic temperature rise, $^{\circ}C$

t   duration of exposure of cylinder, sec

U   local air speed, mph

U'   local air speed, cm/sec

V   true air speed of airplane, mph

w   liquid-water content, g/cu m $(w = 10^6 w')$

w'   liquid-water content, g/cu cm

Z_p pressure-altitude, ft

α_d dry-adiabatic lapse rate, $^\circ C/m$

α_s saturated-adiabatic lapse rate, $^\circ C/m$

μ viscosity of air, $g/(cm)(sec)$

ρ_a density of air, $g/cu\ cm$

ρ_i density of ice, $g/cu\ cm$

ρ_w density of water droplet, $g/cu\ cm$

φ $18\rho_a{}^2 LU'/\mu\rho_w$, dimensionless

Subscripts:

o   volume median

ω weighted average

1,2   cylinders

APPENDIX B

THEORY OF OPERATION

Basic dimensionless parameters. - The mass of ice collected per unit frontal area on a rotating cylinder exposed in a supercooled cloud is given by

$$I' = \frac{m}{2Ll} = EU'w't \tag{B1}$$

where E is the collection efficiency, defined as the ratio of the water in droplet form intercepted by the cylinder to the total amount of water in droplet form in the volume of space swept by the moving cylinder. (All symbols are defined in appendix A.) For clouds composed of droplets of uniform size, the collection efficiency E is given in reference 3 in terms of two dimensionless parameters defined as

$$K \equiv \frac{2}{9} \frac{\rho_w a^2 U'}{\mu L} \tag{B2}$$

and

$$\varphi \equiv \frac{18\rho_a^2 L U'}{\mu \rho_w} \tag{B3}$$

It is assumed that ρ_a, U', and μ do not vary during the exposure period.

When a set of cylinders of different radii is exposed simultaneously from an airplane flying in a supercooled cloud, all of the quantities on the right side of equations (B2) and (B3), with the exception of the cylinder radius L, are the same for each of the cylinders; hence, if L is eliminated by combining equations (B2) and (B3), the resulting parameter

$$K\varphi \equiv \left(\frac{2\rho_a a U'}{\mu}\right)^2 \tag{B4}$$

has the same value for each cylinder of the set. Thus, it is evident that the mathematical condition that $K\varphi$ is a constant corresponds to the physical situation existing during the exposure of a multicylinder set in flight. Moreover, since for a given exposure E is proportional to I' (eq. (B1)) and $1/K$ is proportional to L (eq. (B2)), the functional relation between calculated values of E and $1/K$, when $K\varphi$ is constant, is analogous to the functional relation between the measured

ice collected per unit area and the cylinder radius. This relation provides the basis for comparing the measured weight of ice collected on each of the cylinders with the calculated water-droplet collections for the same cylinders and conditions.

Application of multicylinder method to clouds of nonuniform droplet size. - Because natural clouds are not generally composed of droplets of uniform size, values of average collection efficiency based on nonuniform droplet-size distributions are used for comparing the calculated amounts of ice collected with the measured amounts. Several droplet-size-distribution patterns, presented herein in table III, were adopted in reference 1 to represent what are believed to be some of the characteristic patterns encountered in nature. The droplet size is expressed in the table as the ratio of the average droplet radius in each group to the radius of the volume-median droplet a_0. The amount of water in all droplets of a diameter greater than the volume-median diameter is equal to the amount of water in all the droplets of smaller diameter. A brief explanation of the method for interpreting the table is given with the table.

In a cloud composed of droplets of many different sizes, a cylinder of a given diameter will collect some droplets of every size; however, the collection efficiency with the smaller droplets will be less than with the larger droplets. For each of the assumed droplet-size distributions, such as distribution B in table III, an over-all weighted collection efficiency for a cylinder was calculated in reference 3 by adding the weighted collection efficiencies that are appropriate to each droplet-size group. In the case of distribution B, for example, the collection efficiency pertaining to the volume-median droplet size is assumed to apply to 30 percent of the total water content; 20 percent of the water is assumed to be processed by the cylinder at the lower collection efficiency that applies to droplets with diameters 0.84 as large as the volume-median diameter, and so forth.

The values of the over-all weighted collection efficiency E_ω calculated in this manner are expressed as functions of $1/K_0$ and $K_0\varphi$, where K_0 refers to the volume-median diameter; (K_0 is obtained by substituting a_0 for a in equation (B2)). Values of E_ω from reference 3 are presented in table II for the four selected values of $K_0\varphi$ (200, 1000, 3000, and 10,000), which are herein called standard values.

The correspondence that has been shown to exist between calculated values of the collection efficiency and the ice collected in the case of uniform droplets applies also for nonuniform droplet-size distributions when E and K are replaced by E_ω and K_0. Thus, the relation

between calculated values of E_ω and $1/K_0$, when $K_0\varphi$ is constant, corresponds to the relation between measured amounts of ice collected per unit frontal area and cylinder radius.

Determination of droplet size, liquid-water content, and approximate droplet-size distribution. - The fact that the mass of ice per unit frontal area I' is porportional to E_ω is expressed by the following equation (derived from eq. (B1)), which is written in logarithmic form in order to make the proportionality constant appear as an additive term:

$$\log E_\omega = \log I' - \log U'w't \qquad (B5)$$

Similarly, since LK_0 is the same for all values of L, as shown by equation (B2), the proportionality between $1/K_0$ and L is expressed by the identity

$$\log 1/K_0 \equiv \log L - \log LK_0 \qquad (B6)$$

The additive terms $\log U'w't$ and $\log LK_0$ in equations (B5) and (B6), respectively, permit the translation of the axes of a curve of $\log E_\omega$ as a function of $\log 1/K_0$ with respect to the axes of another curve of $\log I'$ as a function of $\log L$ such that the two curves coincide, provided the physical conditions for which the two curves were obtained are the same.

The flight data are plotted in terms of the coordinates $\log I'$ as a function of $\log L$, as indicated in the section on calculating procedure, and the calculated data of table II are plotted in terms of $\log E_\omega$ and $\log 1/K_0$. The comparison of experimental points and calculated curves is valid if $K_0\varphi$ is approximately the same for both and if the assumed droplet-size distribution applicable to the calculated curve is similar to the actual droplet-size distribution in the cloud. The translation of axes is illustrated in figure 11, in which the data points, which were obtained from actual flight measurements, are plotted in terms of $\log I'$ and $\log L$ with respect to the axes shown by the dashed lines. The theoretical curve of $\log E_\omega$ as a function of $\log 1/K_0$, which applies to droplet-size distribution E (table III) when $K_0\varphi = 3000$ (as shown in fig. 11), is plotted with respect to the axes shown by the solid lines. The vertical axes of the two sets of coordinates are separated by an interval equal to $\log LK_0$, and the horizontal axes are separated by an interval equal to $\log U'w't$. When the plotted points are correctly matched with the calculated curve, the

separation of the axes provides values of log LK_O and log $U'w't$ that
are used to calculate the volume-median droplet radius (eq. (B2)) and the
liquid-water content.

Because the shape of the calculated curves of log E_w as a function
of log $1/K_O$ depends upon the assumed droplet-size distribution, curves
based on the various assumed distributions listed in table III are matched
against the experimental plot of log I' as a function of log L, and
the curve which most closely fits the data points is used in the deter-
mination of liquid-water content and droplet diameter. The assumed
droplet-size distribution corresponding to this chosen curve is taken
as an approximate representation of the degree of homogeniety of the
actual cloud-droplet distribution. If the actual droplet-size distri-
bution in a cloud is not of the same general form as the assumed distri-
butions (e.g., if the distribution is bimodal), the value of droplet
diameter obtained by using the procedure described herein is not neces-
sarily the volume-median diameter. For this reason, some investigators
prefer to use the term "mean-effective diameter" when referring to the
results of multicylinder measurements of droplet size.

In order to fulfill the requirement that approximately the same
value of $K_O\varphi$ must apply to both the experimental and calculated data,
a procedure of successive approximations is necessary. As described in
the section on calculating procedure, an estimated standard value of $K_O\varphi$
is used to determine an approximate value of LK_O, which is used to cal-
culate a corrected value of $K_O\varphi$. The standard value of $K_O\varphi$ that is
nearest to this calculated value is then used in the final determination
of w' and a_O. This procedure is practicable because large errors in
estimating $K_O\varphi$ cause only small changes in LK_O. Since curves are
available for only a few standard values of $K_O\varphi$, the value of $K_O\varphi$ for
the flight data is generally not the same as for the calculated curve.
This difficulty is not serious because the curves of log E_w as a func-
tion of log $1/K_O$ for successive standard values of $K_O\varphi$ are nearly
identical except for a slight displacement in the direction of the axis
of log $1/K_O$. Since this displacement is a known function of $K_O\varphi$, the
value of droplet radius may be corrected by the use of a correction
factor that depends on the corrected value of $K_O\varphi$ and the standard
value applicable to the curve used in determining a_O. This correction
factor is presented in figure 10, which is a graphical means of inter-
polating between the standard values of $K_O\varphi$.

Equations (B1) to (B6) are true with any consistent system of units,
such as those given in the table of symbols. For practical reasons,
certain departures from consistent units are desirable for routine use.

Thus, in the detailed procedure described in the section on calculating procedure, a (rad. in cm) has been replaced by d (diam. in microns), U' (cm/sec) by U (mph), and w' (g/cu cm) by w (g/cu m). Certain numerical conversion factors appear in the calculations because of these changes of units. Also, for routine calculations it is convenient to use logarithmic graph paper for the curve-matching procedure, thus making it unnecessary to use numerical values of the logarithms.

APPENDIX C

ALTERNATE METHOD OF REDUCING ROTATING MULTICYLINDER DATA

By Paul T. Hacker

INTRODUCTION

The method presented in this appendix for the processing of the
flight data to obtain liquid-water content, droplet size, and droplet-
size distribution is identical with the method presented in the body
of the report up to step (f) of Calculating Procedure. The plotting
and matching procedure of steps (f) and (g) are replaced by another
graphical procedure which eliminates the necessity of making a series
of successive approximations to the value of $K\varphi$. (Symbols are defined
in appendix A.) This method directly yields two quantities: $K\varphi$, from
which the droplet size is computed; and $1/Utw$, which is proportional
to the liquid-water content. Theoretically, approximate droplet-size-
distribution patterns can also be obtained by this method by using the
calculated impingement data for various assumed droplet-distribution
patterns presented in table II. The theory of the method is presented,
and a stepwise calculating procedure is outlined. The stepwise pro-
cedure is illustrated with the same example used for the method pre-
sented in the body of the report.

THEORY OF METHOD

Basic concepts, assumptions, and dimensionless parameters. - The
basic concepts, assumptions, and dimensionless parameters for this
method are identical with those used for the standard method. The mass
of ice collected per unit frontal area on a rotating cylinder exposed
in a supercooled cloud is given by

$$I' = \frac{m}{2L\mathit{l}} = EU'w't \tag{B1}$$

where L is the average radius of the iced cylinder and E is the
collection efficiency which corresponds to the average radius. For
clouds composed of droplets of uniform size, the theoretical collection
efficiency E is given in reference 3 in terms of two dimensionless
parameters defined as

$$K \equiv \frac{2}{9} \frac{\rho_w a^2 U'}{\mu L} \tag{B2}$$

and

$$\varphi \equiv \frac{18\rho_a{}^2 LU'}{\mu\rho_w} \tag{B3}$$

The data for uniform droplet size (distribution A) are reproduced in
this report in table II.

If equations (B2) and (B3) are combined by multiplying, the result

$$K\varphi \equiv \left(\frac{2\rho_a aU'}{\mu}\right)^2 \tag{B4}$$

is a new dimensionless parameter which does not contain the cylinder
size. The mathematical condition that $K\varphi$ is a constant corresponds
to the physical situation existing during the exposure of a multicylinder
set in flight, and the only unknown quantity is the droplet radius a
for any given exposure. Since $K\varphi$ is constant for all cylinders for a
given exposure, it is convenient to express the theoretical collection-
efficiency data of table II in terms of $K\varphi$ and φ. Figure 12(a) is a
plot of the collection efficiency E as a function of φ for various
values of $K\varphi$ for droplets of uniform size (distribution A). This plot
is the working chart for this method of determining droplet size and
liquid-water content.

Determination of liquid-water content and droplet size. - For
droplets of uniform size it is theoretically possible to determine by
this method the droplet size and liquid-water content from the amount
of ice collected on two cylinders of different diameters. For practical
purposes, however, several cylinders should be employed in order to
eliminate errors in droplet size and liquid-water content due to errors
in the measured amount of ice collected on a cylinder. Only two cylin-
ders will be used, however, to develop the theory of the method.

Assume that two cylinders with initial radii of $L_{0,1}$ and $L_{0,2}$
are exposed for a period of time t and collect amounts of ice m_1
and m_2, respectively. Average radii (L_1 and L_2) may be calculated
for the two cylinders by the equation

$$L = \frac{1}{2}\left(L_0 + \sqrt{\frac{m}{\rho_i \pi l} + L_0{}^2}\right) \tag{C1}$$

from which two values of φ (φ_1 and φ_2) may be calculated by equa-
tion (B3) and other flight data. Substitution of values of mass of ice

collected m and average cylinder radius L into equation (B1) gives

$$I_1 = \frac{m_1}{L_1 l} = E_1 U'w't \qquad (C2)$$

and

$$I_2 = \frac{m_2}{L_2 l} = E_2 U'w't \qquad (C3)$$

where E_1, E_2, and w' are unknown quantities; but w', the liquid-water
content, is the same for the two cylinders. Since L is the only factor
that changes the value of φ for any given exposure, equation (C2) is
for $\varphi = \varphi_1$ and equation (C3) is for $\varphi = \varphi_2$. Solving the two equations
for 1/U'w't gives

$$\frac{1}{U'w't} = \frac{E_1}{I_1} \qquad (C4)$$

and

$$\frac{1}{U'w't} = \frac{E_2}{I_2} \qquad (C5)$$

The right side of the two expressions may be set equal to each other
because U'w't is identical for both. The result is

$$\frac{E_1}{I_1} = \frac{E_2}{I_2} \qquad (C6)$$

where $\varphi = \varphi_1$ for the left side and $\varphi = \varphi_2$ for the right side. Equa-
tion (C6) states that the ratio of collection efficiency to the mass of
ice collected per unit frontal area is the same for all cylinders for a
given exposure. Equation (C6) is the fundamental relation upon which
this method is based.

From figure 12(a) it is possible to determine a value of $K\varphi$ which
is constant for a given exposure of cylinders so that the ratio of the
collection efficiency to the mass of ice collected per unit frontal area
is the same for all values of φ (in this case φ_1 and φ_2). This
determination is accomplished in the following manner: For a constant
value of φ, say φ_1, the theoretical values of E are tabulated from
figure 12(a) for various values of $K\varphi$. The values of E are then
divided by the mass per unit frontal area of the cylinder I_1, and a
plot of $K\varphi$ as a function of E/I_1 is made. The same procedure is

used for φ_2, and the results are plotted on the same chart as those for φ_1. Curves are faired through the two sets of points, and the point of intersection of the two curves determines the value of $K\varphi$ for which equation (C6) is satisfied. From this value of $K\varphi$ the droplet size can be calculated by use of equation (B4). The intersection point also determines a value of E/I from which the liquid-water content w' can be determined by equations (C4) or (C5), since U' and t are known.

When three or more cylinders are employed, all the curves of $K\varphi$ against E/I should intersect in a point. If there are errors in the amounts of ice collected on individual cylinders or the cloud is not composed of droplets of uniform size, then the curves will not intersect in a point.

Application of method to clouds of nonuniform droplet size. - Theoretically, this method may be used to determine approximate droplet-size-distribution patterns if working charts (fig. 12(a)) are made for the various assumed droplet distributions presented in table III. Working charts for distributions C and E are shown in figures 12(b) and 12(c), respectively. Three or more cylinders are required to determine the droplet-size distribution. The experimental data are processed for all assumed droplet-size distributions, and the one that most nearly gives a single intersection point for the $K\varphi$ against E/I curves is the approximate droplet-size distribution. As was discussed in appendix B, the droplet size is the mean-effective droplet size, the collection efficiency is the weighted collection efficiency E_w, and K in $K\varphi$ is replaced by K_0 for the mean-effective droplet size.

Units for equations. - The preceding equations are true for any consistent system of units, such as those given in appendix A. For practical reasons certain departures from consistent units are desirable for routine use. Thus, in the detailed calculation procedure described in the following section, mixed units will be employed. As a result, numerical conversion factors will appear in the calculations.

STEPWISE CALCULATING PROCEDURE

Steps (a) to (e) in the calculation procedure for this method are identical with those in the body of the report, and the various items entered in the work sheet, table I, are also identical through item (15). A work sheet for this alternate method with an actual observation as an example is presented in table IV.

Step (f): Calculation of φ for average radii of cylinders. - The parameter φ is calculated for each cylinder by use of the average

radius L (item (14)), U (item (3)), and φ/LU (item (9)). The
values of φ for the example are 237, 690, 1608, 3765, and 5638 for
the five cylinders. These values are entered as item (16) in table IV
and indicated by horizontal lines on figure 12.

Step (g): Tabulation of E_ω as function of $K_0\varphi$ for values of
φ computed in step (f). - Tabulated values of E_ω (E_ω is identical
to E for distribution A) as a function of $K_0\varphi$ for the values of φ
computed in step (f) are obtained from figure 12 by reading the value
of E_ω for the intersection points of a constant φ line with the
$K_0\varphi$ curves. For example, for $\varphi = 237$ (fig. 12(a)), the values of
E_ω for $K_0\varphi$ equal to 200, 1000, 3000 and 10,000 are 0.253, 0.678,
0.844, and 0.913, respectively. If the droplet-size distribution is
to be determined, it is necessary to tabulate E_ω as a function of
$K_0\varphi$ with φ constant for all the assumed droplet-size distributions.
The values of $K_0\varphi$ and E_ω thus obtained are entered in columns I
and II, respectively, of item (17) of table IV for the appropriate
cylinder size and droplet-size distribution.

Step (h): Calculation of E_ω/I. - The values of E_ω for the
various cylinders entered in columns II of item (17) are divided by
the corresponding value of I (item (15)), and the results are
entered in columns III of item (17).

Step (i): Plotting $K_0\varphi$ as a function of E_ω/I. - For a given
assumed droplet-size distribution, the values of $K_0\varphi$ (column I,
item (17)) are plotted as a function of E_ω/I (columns III, item (17))
for all cylinders on a single sheet of semilog paper. Curves are faired
through the plotted points as shown in figure 13. The curves should
intersect in a point, if the correct droplet-size distribution has been
assumed and there are no errors in the amount of ice collected on an
individual cylinder. If the curves do not intersect in a single point
for any droplet-size distribution, the midpoint of the smallest polygon
formed by the intersecting curves is used to determine $K_0\varphi$ and E_ω/I.
An inspection of figure 13 reveals that for the example the curves
for distribution E (fig. 13(c)) most nearly intersect in a point. This
droplet-size distribution is entered as item (18) of table IV. At the
intersection point the values of $K_0\varphi$ and E_ω/I are read and entered
as items (19) and (20) of table IV. These values are 5400 and
8.46×10^{-5}, respectively.

Step (j): Determination of droplet size   d. - The droplet size is
determined from the value of $K_0\varphi$ (item (19)) and the following
equation:

$$d = \frac{\mu\sqrt{K_0\varphi}}{4.8\times10^{-6}(\rho_a U)}$$

which is derived from the definition of $K\varphi$ given as equation (B4).
Values of viscosity μ and air density ρ_a which correspond to the
·corrected air temperature T (item (7)) and the pressure-altitude Z_p
(item (4)),· respectively, may be found in many references. Another
method for finding the droplet size is to convert $K_0\varphi$ into LK_0 by
items (14) and (16) and use the graphical method presented in figure 9.
For the example, the droplet size is 14.1 microns and is entered as
item (21) of table IV.

Step (k): Determination of liquid-water content w. - The liquid-
water content is determined from the value of the quantity E_ω/I deter-
mined in step (i). This value of E_ω/I, which was determined by the
intersection point of the curves of $K_0\varphi$ against E_ω/I, is actually
equal to $1/Utw$. The liquid-water content is determined by dividing the
reciprocal of $1/Utw$ by the product of U (item (3)) and t (item (8)).
The liquid-water content for the example is 0.30 gram per cubic meter;
this value is entered as item (22) of table IV.

DISCUSSION OF METHOD

A comparison of the end results by this method (items (18), (21),
and (22) of table IV) with those obtained by the standard method
(items (20), (23), and (24), of table I) shows very good agreement for
the liquid-water content, droplet size, and droplet-size distribution.
Droplet-size distribution E, however, may not be true for either method,
because the curve of $K_0\varphi$ against E_ω/I for the $4\frac{1}{2}$-inch cylinder did
not intersect in a point with the other curves. For other sample cal-
culations of actual flight data not presented here, the agreement was
not always as good. This was especially true for droplet-size distribu-
tion. For liquid-water content and droplet size, the maximum difference
was of the order of 10 percent. From these sample calculations some
points of interest were observed as follows:

(1) The curves of $K_0\varphi$ against E_ω/I for the 1/8-inch cylinder
very often did not intersect in the same points as the other curves for
any droplet-size distribution. This was especially true when the amount
of ice collected by the 1/8-inch cylinder was large (diameter doubling
during exposure time).

(2) The curves of $K_0\varphi$ against E_ω/I for the 1/2-, $1\frac{1}{4}$-, and 3-inch cylinders usually intersected in a small area for any droplet-distribution pattern (see fig. 13).

(3) For some flight data, no more than two curves of $K_0\varphi$ against E_ω/I ever intersected in a point for any assumed droplet-size distribution.

The intersection of all the curves of $K_0\varphi$ against E_ω/I in a single point for a given droplet-size distribution by this method is identical to all the plotted points falling along the given size-distribution curve by the standard method. However, droplet-size distribution determinations are unreliable by either method because an error in the amount of ice collected by one or more cylinders will give a droplet-size distribution which does not exist.

This method requires more calculations and plotting than the standard method. However, it eliminates the necessity of making approximations to the value of $K_0\varphi$ and the matching of plotted points to standard curves by moving one chart with respect to the other. Therefore, this method may be more easily used and understood by inexperienced personnel than the standard method.

REFERENCES

1. Langmuir, Irving, and Blodgett, Katherine B.: A Mathematical Investigation of Water Droplet Trajectories. Tech. Rep. No. 5418, Air Materiel Command, AAF, Feb. 19, 1946. (Contract No. W-33-038-ac-195⊥ with General Electric Co.)

2. Anon.: The Multicylinder Method. The Mount Washington Monthly Res. Bull., vol. II, no. 6, June 1946.

3. Brun, Rinaldo J., and Mergler, Harry W.: Impingement of Water Droplets on a Cylinder in an Incompressible Flow Field and an Evaluation of Rotating Multicylinder Method for Measurement of Droplet-Size Distribution, Volume-Median Droplet Size, and Liquid-Water Content in Clouds. NACA TN 2904, 1953.

4. Howell, Wallace E.: Comparison of Three Multicylinder Icing Meters and Critique of Multicylinder Method. NACA TN 2708, 1952.

5. Neel, Carr B., Jr., Bergrun, Norman R., Jukoff, David, and Schlaff,
      Bernard A.: The Calculation of the Heat Required for Wing Thermal
      Ice Prevention in Specified Icing Conditions. NACA TN 1472, 1947.

6. Fraser D., Rush, C. K., and Baxter, D.: Thermodynamic Limitations of
      Ice Accretion Instruments. Lab. Rep. LR-32, National Aeronautical
      Establishment, Ottawa (Canada), August 22, 1952.

TABLE I. - WORK SHEET WITH SAMPLE DATA FROM AN ACTUAL OBSERVATION

(1) Average indicated air speed, mph   171
(2) Average true air speed, mph   185
(3) Average local air speed, U, mph   185
(4) Pressure-altitude, Z_p, ft 7000
(5) Uncorrected air temperature, °C . . . . -10.1
(6) Wet-air temperature correction, °C . . . .   -2.1
(7) Corrected temperature, T, °C . . . . -12.2
(8) Exposure period, t, sec   216
(9) φ/LU, hr/(mile)(cm). 5.3

	Cylinder diameter, in.				
	$\frac{1}{8}$	$\frac{1}{2}$	$1\frac{1}{4}$	3	$4\frac{1}{2}$
	Cylinder radius, L_0, cm				
	0.15875	0.6350	1.5875	3.810	5.715
(10) Gross weight, g	7.44	23.56	59.68	141.83	190.47
(11) Tare weight, g	6.34	20.94	55.16	135.61	183.41
(12) Net weight, g	1.10	2.62	4.52	6.22	7.06
(13) Corrected net weight, g	1.10	2.62	4.52	6.22	7.06
(14) L, cm	0.242	0.704	1.64	3.84	5.75
(15) I, (miles/hr)(sec)(g/cu m)	9980	8190	6070	3570	2700

	A Preliminary estimate	B First approximation	C Final values
(16) $K_0\varphi$ (nearest standard)	3000	3000	-----
(17) LK_0, cm	----,	4.90	-----
(18) $K_0\varphi$ (corrected)	----	4800	-----
(19) Droplet diameter (uncorrected) microns	----	----	13.3
(20) Droplet-size distribution (letter)	----	E	-----
(21) Utw, (miles/hr)(sec)(g/cu m)	----	11,900	-----

(22) Droplet-diameter correction factor 1.033
(23) Mean-effective droplet diameter, d, microns 13.7
(24) Liquid-water content, w, g/cu m 0.30

TABLE II. - CALCULATED VALUES OF CYLINDER COLLECTION EFFICIENCY

FOR STANDARD VALUES OF $K_O \varphi$

[Data from ref. 3.]

	A		B		C		D		E
$1/K_O$	E_ω	$0.6E_\omega$	E_ω	$0.7E_\omega$	E_ω	$0.8E_\omega$	E_ω	$0.9E_\omega$	E_ω
				$K_O \varphi = 200$					
4.00	0.027	0.016	0.039	0.027	0.050	0.040	0.066	0.059	0.083
2.00	.135	.081	.138	.097	.146	.117	.165	.149	.182
1.00	.298	.179	.302	.211	.306	.245	.315	.284	.319
.50	.493	.296	.486	.340	.482	.386	.480	.432	.477
.20	.761	.457	.740	.518	.721	.577	.703	.633	.686
.10	.874	.524	.859	.601	.846	.677	.826	.743	.805
.05	.925	.555	.919	.643	.910	.728	.901	.811	.878
.02	.960	.576	.959	.671	.955	.764	.948	.853	.938
.01	.976	.586	.975	.683	.976	.781	.971	.874	.963
				$K_O \varphi = 1000$					
4.00	0.019	0.011	0.029	0.020	0.038	0.030	0.050	0.045	0.065
2.00	.109	.065	.109	.076	.122	.098	.138	.124	.154
1.00	.251	.151	.252	.176	.259	.207	.271	.244	.283
.50	.460	.276	.452	.316	.423	.338	.447	.402	.447
.20	.714	.428	.697	.488	.677	.542	.661	.595	.643
.10	.830	.498	.816	.571	.800	.640	.783	.705	.763
.05	.908	.545	.899	.629	.892	.714	.876	.788	.862
.02	.953	.572	.953	.667	.949	.759	.943	.849	.933
.01	.971	.583	.972	.680	.973	.778	.967	.870	.962

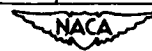## TABLE II. - CALCULATED VALUES OF CYLINDER COLLECTION EFFICIENCY

FOR STANDARD VALUES OF $K_O \varphi$ - Concluded

[Data from ref. 3.]

$1/K_O$	A		B		C		D		E
	E_ω	$0.6E_\omega$	E_ω	$0.7E_\omega$	E_ω	$0.8E_\omega$	E_ω	$0.9E_\omega$	E_ω
$K_O \varphi = 3000$
4.00	0.013	0.008	0.020	0.014	0.027	0.022	0.039	0.035	0.048
2.00	.085	.051	.090	.063	.100	.080	.111	.100	.130
1.00	.218	.131	.225	.158	.235	.188	.244	.220	.251
.50	.409	.245	.416	.291	.410	.328	.415	.374	.413
.20	.687	.412	.668	.468	.652	.522	.641	.577	.623
.10	.815	.489	.797	.558	.785	.628	.766	.689	.746
.05	.884	.530	.878	.615	.867	.694	.855	.770	.839
.02	.945	.567	.940	.658	.938	.750	.921	.829	.918
.01	.968	.581	.966	.676	.970	.776	.964	.868	.954
$K_O \varphi = 10,000$
4.00	0.008	0.005	0.013	0.009	0.017	0.014	0.023	0.021	0.034
2.00	.057	.034	.060	.042	.072	.058	.083	.075	.092
1.00	.157	.094	.163	.114	.172	.138	.188	.169	.202
.50	.350	.210	.356	.249	.357	.286	.362	.326	.368
.20	.645	.387	.630	.441	.615	.492	.599	.539	.591
.10	.778	.467	.764	.535	.748	.598	.731	.658	.713
.05	.865	.519	.857	.600	.849	.679	.830	.747	.816
.02	.920	.552	.920	.644	.918	.734	.909	.818	.899
.01	.952	.571	.950	.665	.955	.764	.946	.851	.939

TABLE III. - FIVE ASSUMED DISTRIBUTIONS OF DROPLET SIZE

[Data from ref. 1]

Liquid-water content in each group size, percent	Distributions				
	A	B	C	D	E
	a/a_O				
5	1.00	0.56	0.42	0.31	0.23
10	1.00	.72	.61	.52	.44
20	1.00	.84	.77	.71	.65
30	1.00	1.00	1.00	1.00	1.00
20	1.00	1.17	1.26	1.37	1.48
10	1.00	1.32	1.51	1.74	2.00
5	1.00	1.49	1.81	2.22	2.71

The size is expressed as the ratio of the average droplet radius in each group to the volume-median droplet radius a_O.

Example of interpretation: 30 percent of the liquid-water content of any cloud is contained in droplets which have a radius a_O. In the case of the B-distribution, 20 percent of the liquid-water content is contained in droplets which have a radius smaller than the volume-median radius a_O by a ratio $a/a_O = 0.84$ and another 20 percent in droplets which have a radius larger than a_O by a ratio $a/a_O = 1.17$. A similar interpretation applies to the remaining values.

TABLE IV. - WORK SHEET FOR ALTERNATE METHOD WITH AN

ACTUAL OBSERVATION AS AN EXAMPLE

(1) Average indicated air speed, mph 171
(2) Average true air speed, mph 185
(3) Average local air speed, U, mph 185
(4) Pressure-altitude, Z_p, ft 7000
(5) Uncorrected air temperature, $^\circ$C . . . . -10.1
(6) Wet-air temperature correction, $^\circ$C . . . . -2.1
(7) Corrected temperature, T, $^\circ$C . . . . -12.2
(8) Exposure period, t, sec 216
(9) φ/LU, hr/(mile)(cm) 5.3

	Cylinder diameter, in.				
	$\frac{1}{8}$	$\frac{1}{2}$	$1\frac{1}{4}$	3	$4\frac{1}{2}$
	Cylinder radius, L_0, cm				
	0.15875	0.6350	1.5875	3.810	5.715
(10) Gross weight, g	7.44	23.56	59.68	141.83	190.47
(11) Tare weight, g	6.34	20.94	55.16	135.61	183.41
(12) Net weight, g	1.10	2.62	4.52	6.22	7.06
(13) Corrected net weight, g	1.10	2.62	4.52	6.22	7.06
(14) L, cm	0.242	0.704	1.64	3.84	5.75
(15) I, (miles/hr)(sec)(g/cu m)	9980	8190	6070	3570	2700
(16) φ, dimensionless	237	690	1608	3765	5638

TABLE IV. – WORK SHEET FOR ALTERNATE METHOD WITH AN ACTUAL OBSERVATION AS AN EXAMPLE – Concluded

(17) Initial cylinder diameter, in.										
$\frac{1}{8}$			$\frac{1}{2}$		$1\frac{1}{4}$		3		$4\frac{1}{2}$	
237			690		1680		3765		5638	

φ for average diameters of iced cylinder

I	II	III	II	III	II	III	II	III	II	III
$K_0\varphi$	E_ω	E_ω/I	E_ω	E_ω/I	E_ω	E_ω/I	E_ω	E_ω/I	E_ω	E_ω/I

Distribution A

$K_0\varphi$	E_ω	E_ω/I	E_ω	E_ω/I	E_ω	E_ω/I	E_ω	E_ω/I	E_ω	E_ω/I
200	0.253	2.53×10^{-5}	0.046	0.56×10^{-5}	0	2.43×10^{-5}	0	$.64\times10^{-5}$	0	$.22\times10^{-5}$
1,000	.678	6.78	.357	4.36	.150	6.33	.023	4.59	.006	3.52
3,000	.844	8.44	.653	7.75	.390	11.24	.164	12.28	.095	11.60
10,000	.913	9.13	.830	10.13	.694	11.24	.438	12.28	.313	11.60

Distribution C

$K_0\varphi$	E_ω	E_ω/I	E_ω	E_ω/I	E_ω	E_ω/I	E_ω	E_ω/I	E_ω	E_ω/I
200	0.261	2.61×10^{-5}	0.068	0.83×10^{-5}	0	2.62×10^{-5}	0	1.26×10^{-5}	0	$.56\times10^{-5}$
1,000	.640	6.40	.346	4.22	.159	6.48	.045	5.10	.015	4.07
3,000	.816	8.16	.621	7.58	.393	10.92	.182	12.44	.110	11.90
10,000	.906	9.06	.808	9.88	.663	10.92	.444	12.44	.321	11.90

Distribution E

$K_0\varphi$	E_ω	E_ω/I	E_ω	E_ω/I	E_ω	E_ω/I	E_ω	E_ω/I	E_ω	E_ω/I
200	0.282	2.82×10^{-5}	0.102	1.24×10^{-5}	0	3.12×10^{-5}	0	1.96×10^{-5}	0	1.73×10^{-5}
1,000	.611	6.11	.366	4.47	.189	6.48	.070	5.74	.029	5.18
3,000	.781	7.81	.595	7.26	.393	10.42	.205	12.49	.140	12.49
10,000	.888	8.88	.772	9.43	.632	10.42	.446	12.49	.337	12.49

(18) Droplet-size distribution (letter) . . . . E

(19) $K_0\varphi$ 5400

(20) $E_\omega/I = 1/Utw$ . . . . 8.46×10^{-5}

(21) Mean-effective droplet diameter, d, microns 14.1

(22) Liquid-water content, w, g/cu m 0.30
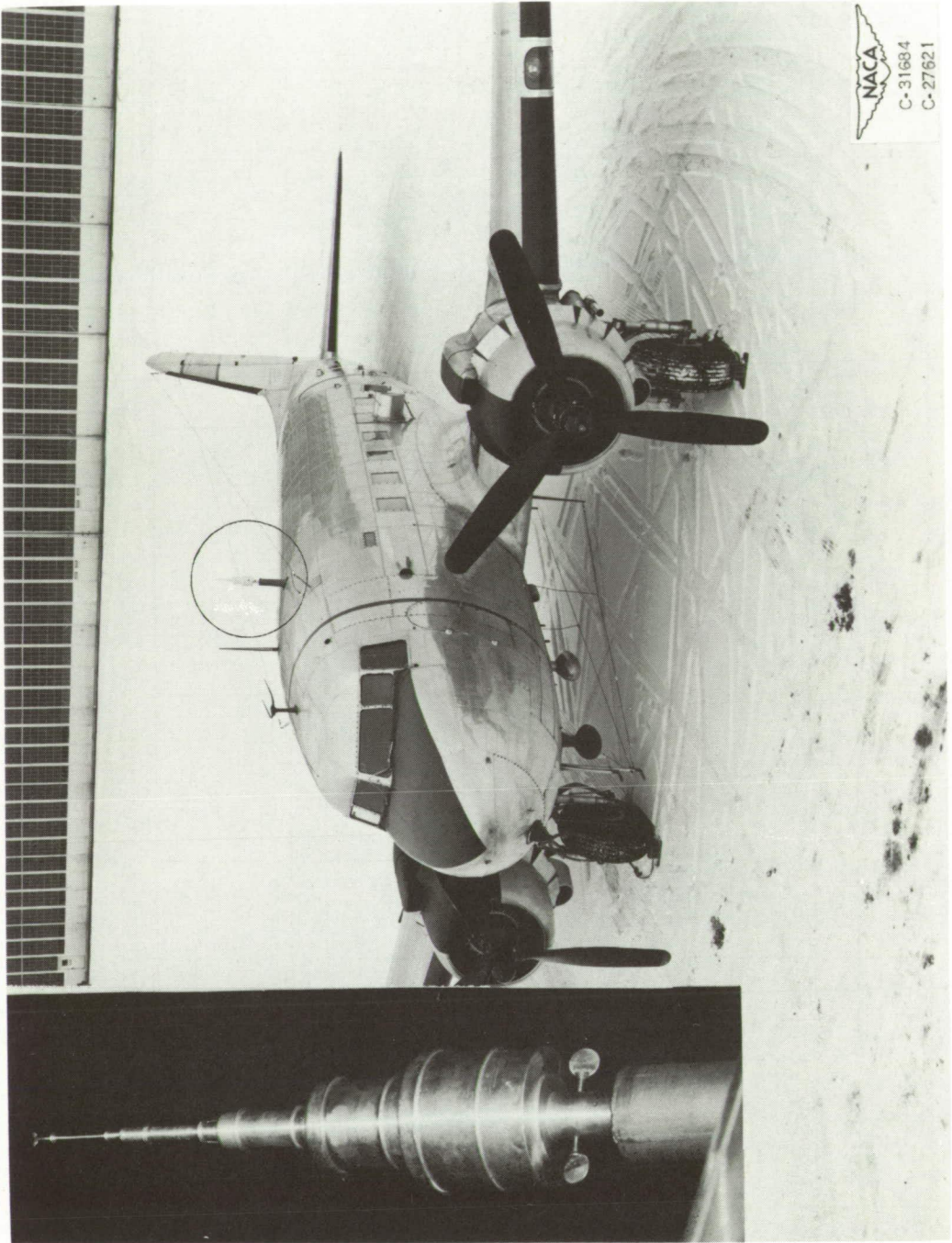
Figure 1. - Rotating multicylinder set extended through top of airplane fuselage.
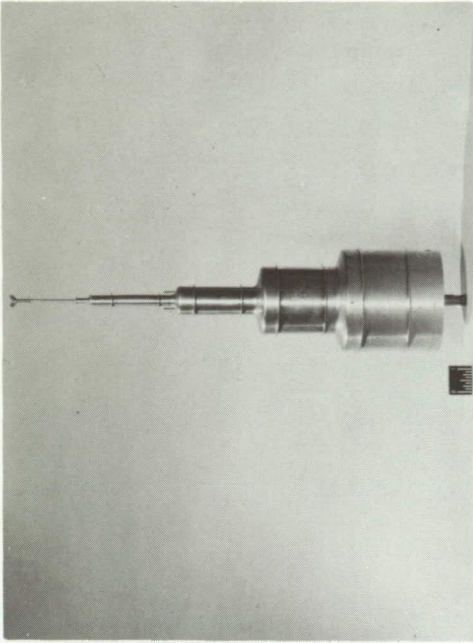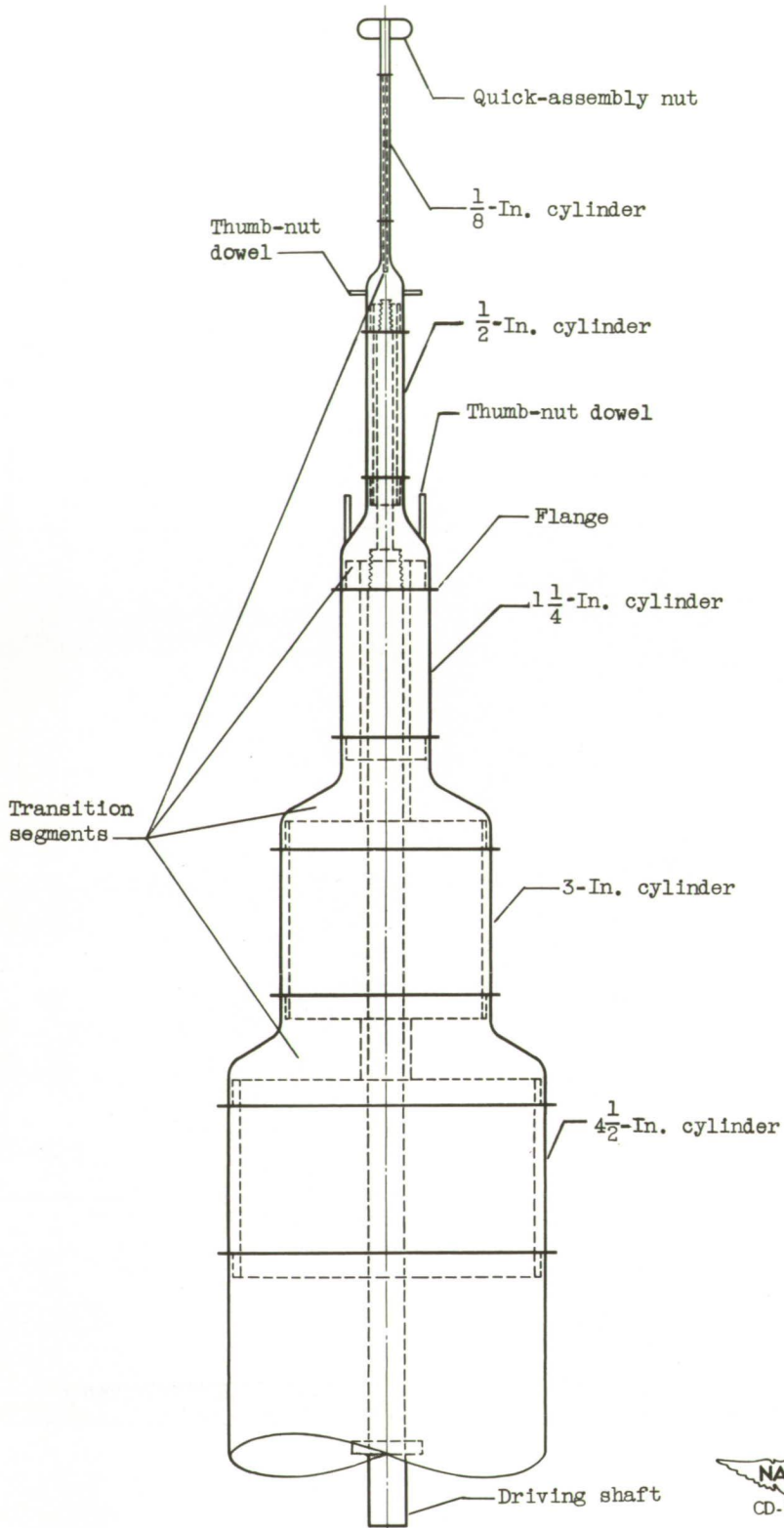
Assembled set of cyclinders
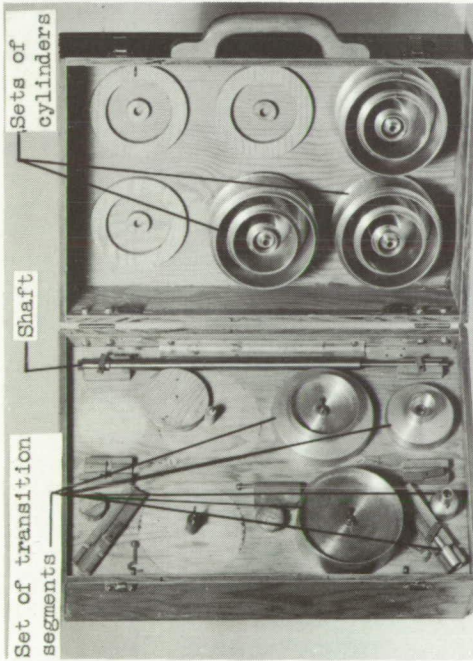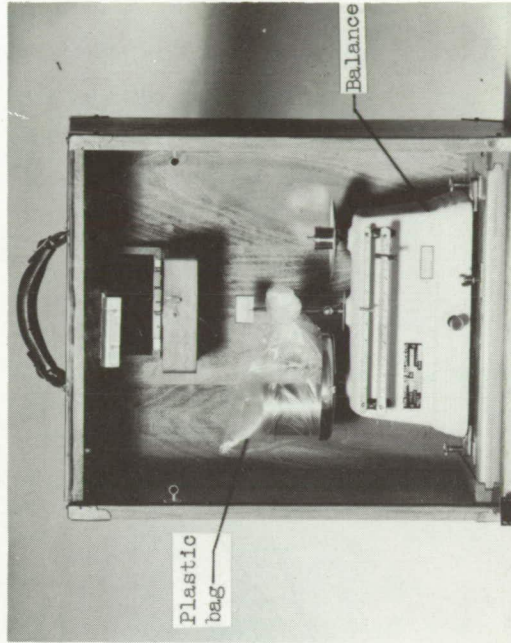
Balance case
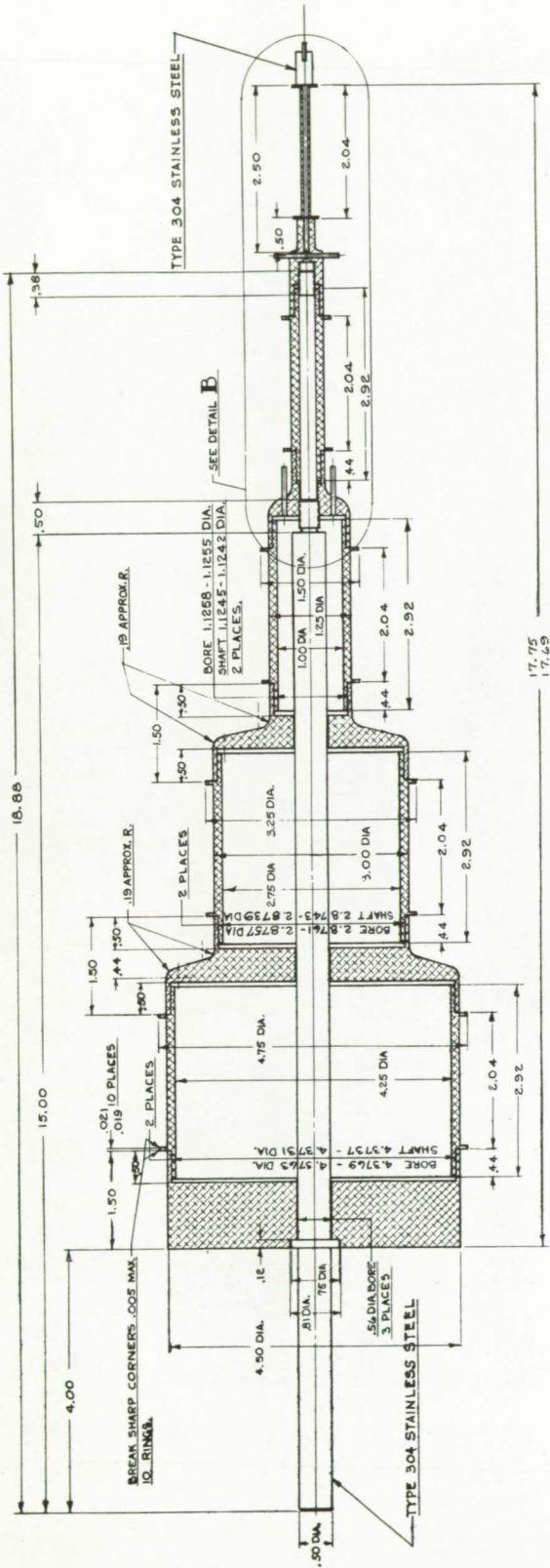
Carrying case
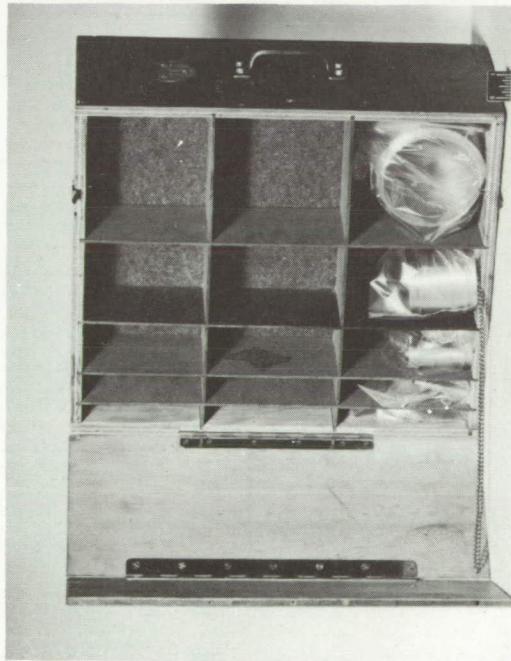
Storage case

Figure 2. - Multicylinder kit.

Quick-assembly nut

$\frac{1}{8}$-In. cylinder

Thumb-nut dowel

$\frac{1}{2}$-In. cylinder

Thumb-nut dowel

Flange

$1\frac{1}{4}$-In. cylinder

Transition segments

3-In. cylinder

$4\frac{1}{2}$-In. cylinder

Driving shaft

CD-2142

(a) Assembly sketch.

Figure 3. - Assembled set of cylinders.
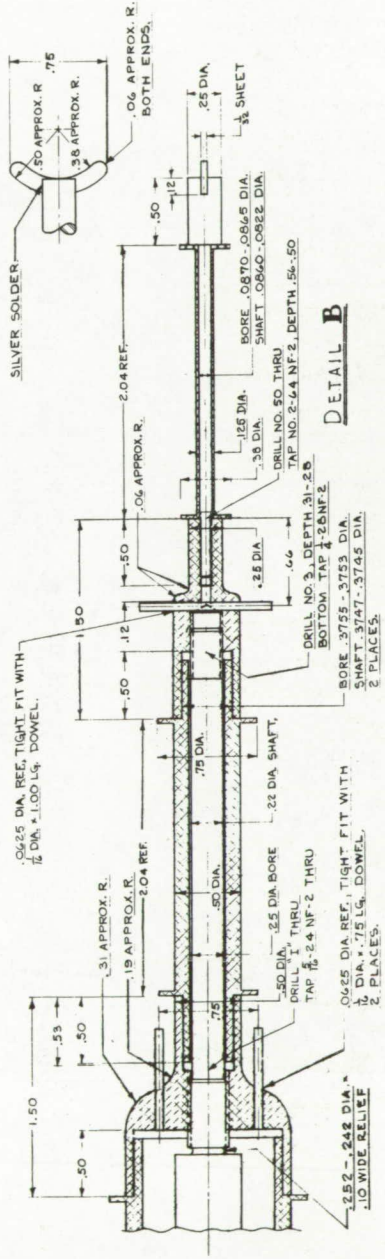
(b) Detailed drawings. (All dimensions are in inches.)

Figure 3. - Concluded. Assembled set of cylinders.
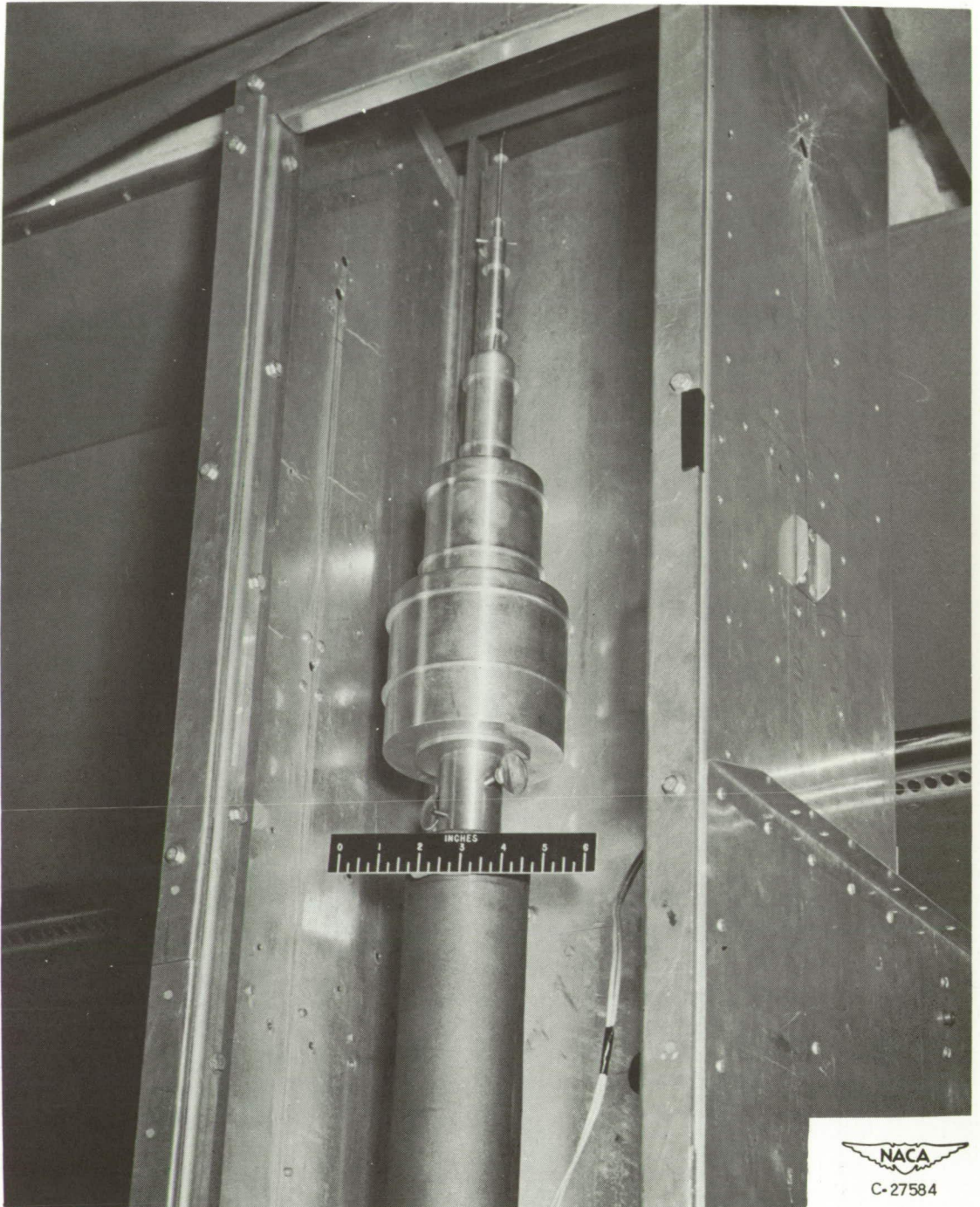
Figure 4. - Assembled set of cylinders mounted in extending and supporting frame.
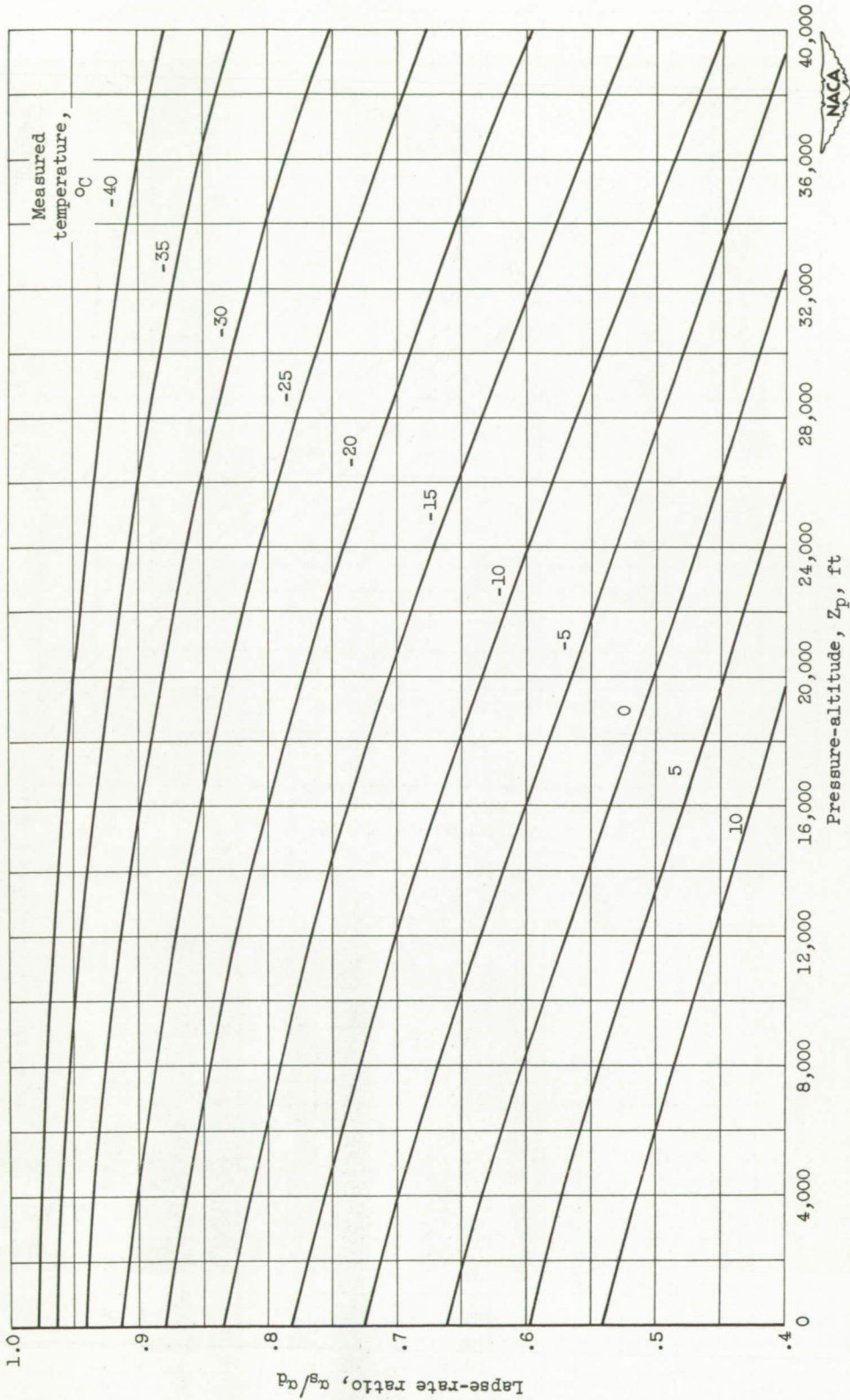
Figure 5. - Ratio of saturated- to dry-adiabatic lapse rate as function of temperature and pressure-altitude.
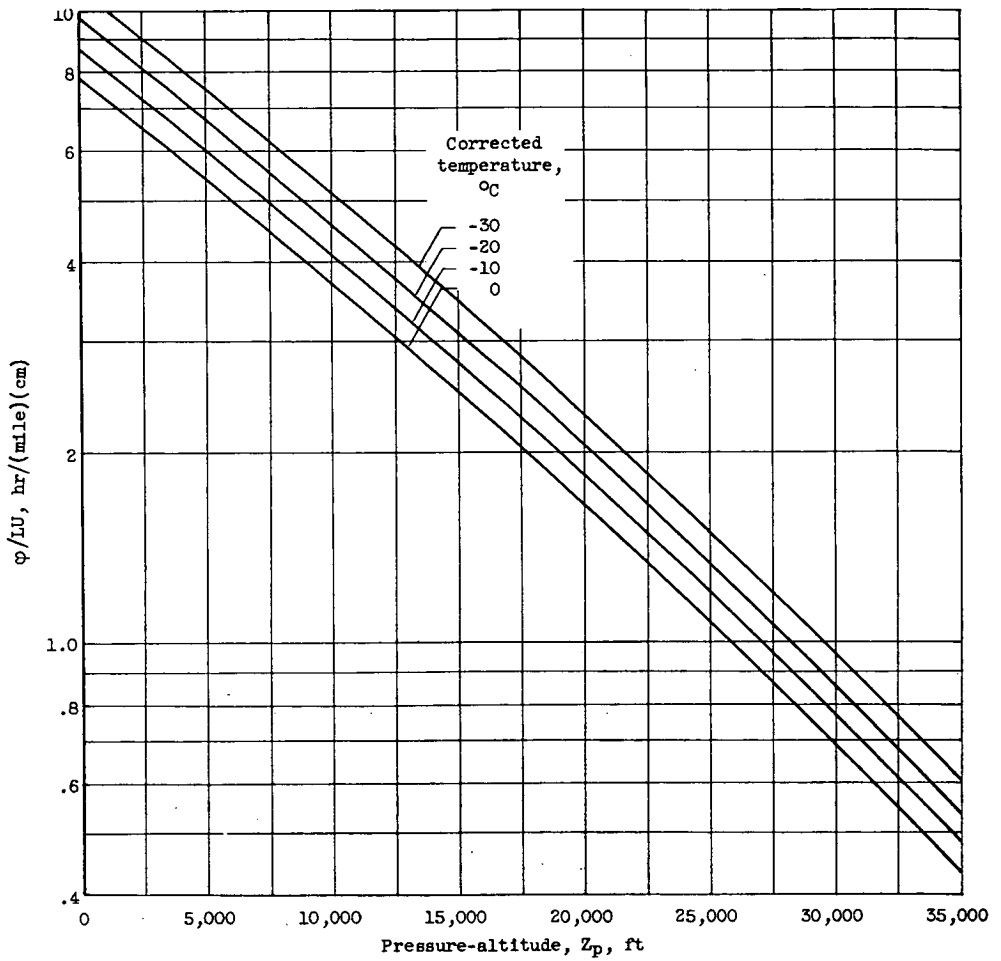
Figure 6. - Parameter φ/LU as function of temperature and pressure-altitude.
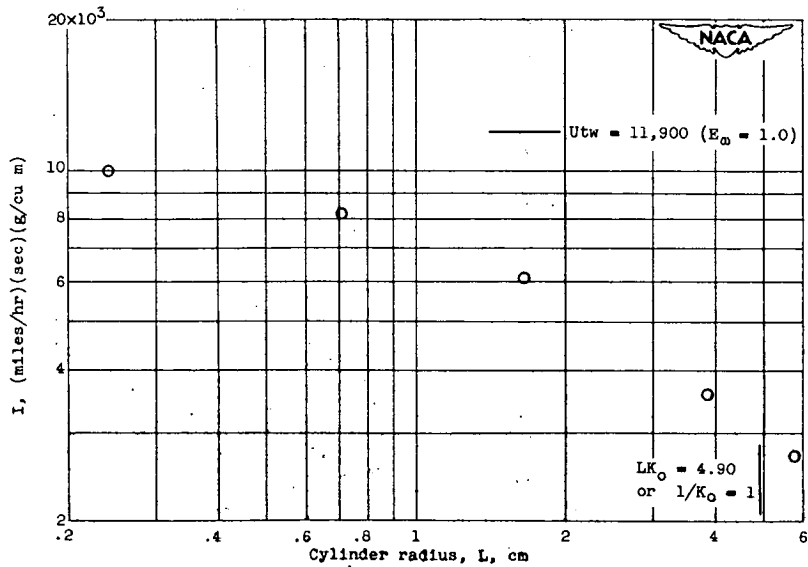
Figure 7. - Sample plot of I as function of cylinder radius.
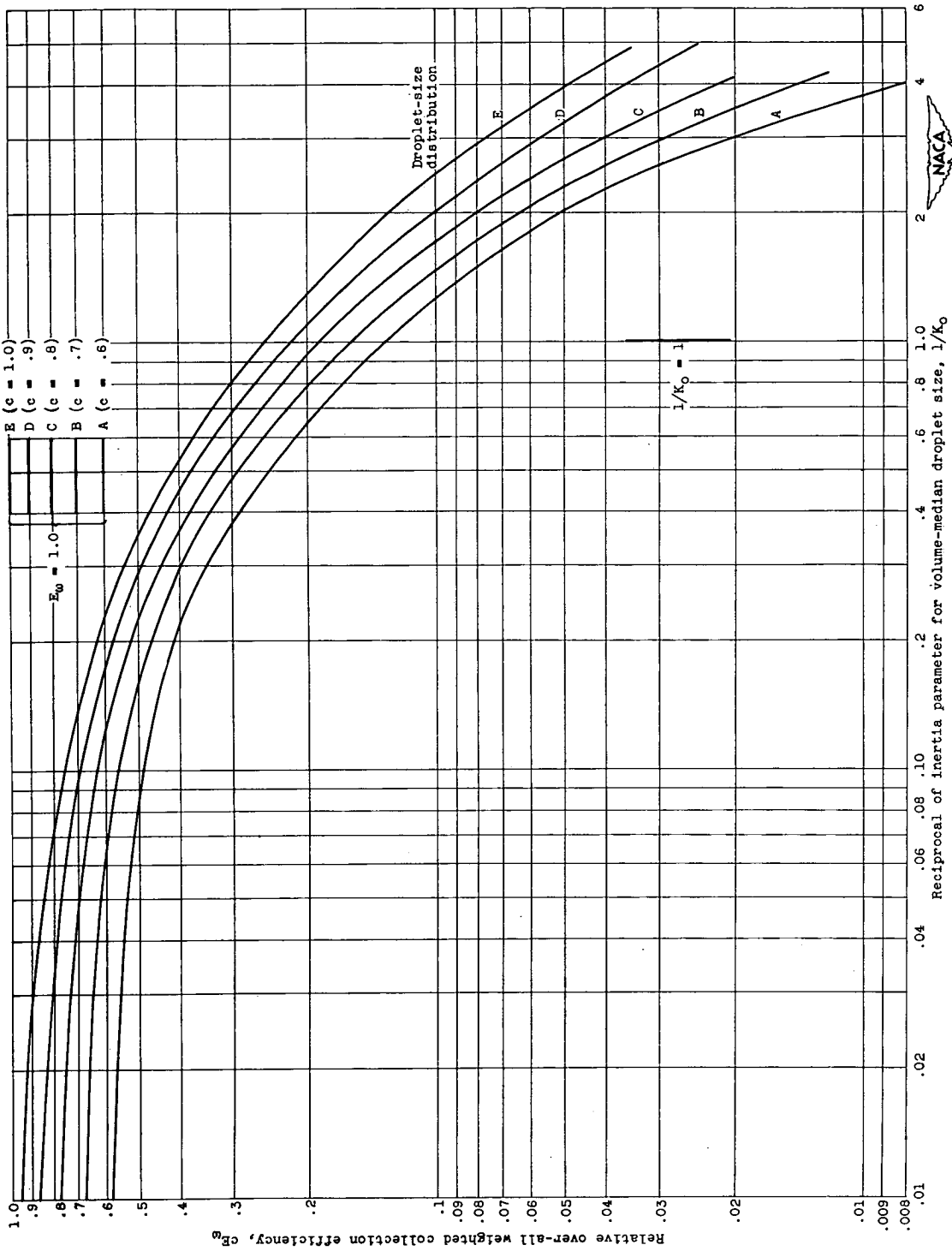
Figure 8. – Curves from data of table II showing relative over-all weighted collection efficiency as function of reciprocal of inertia parameter for $K_0\varphi$ = 3000 for droplet-size distributions defined in table III.
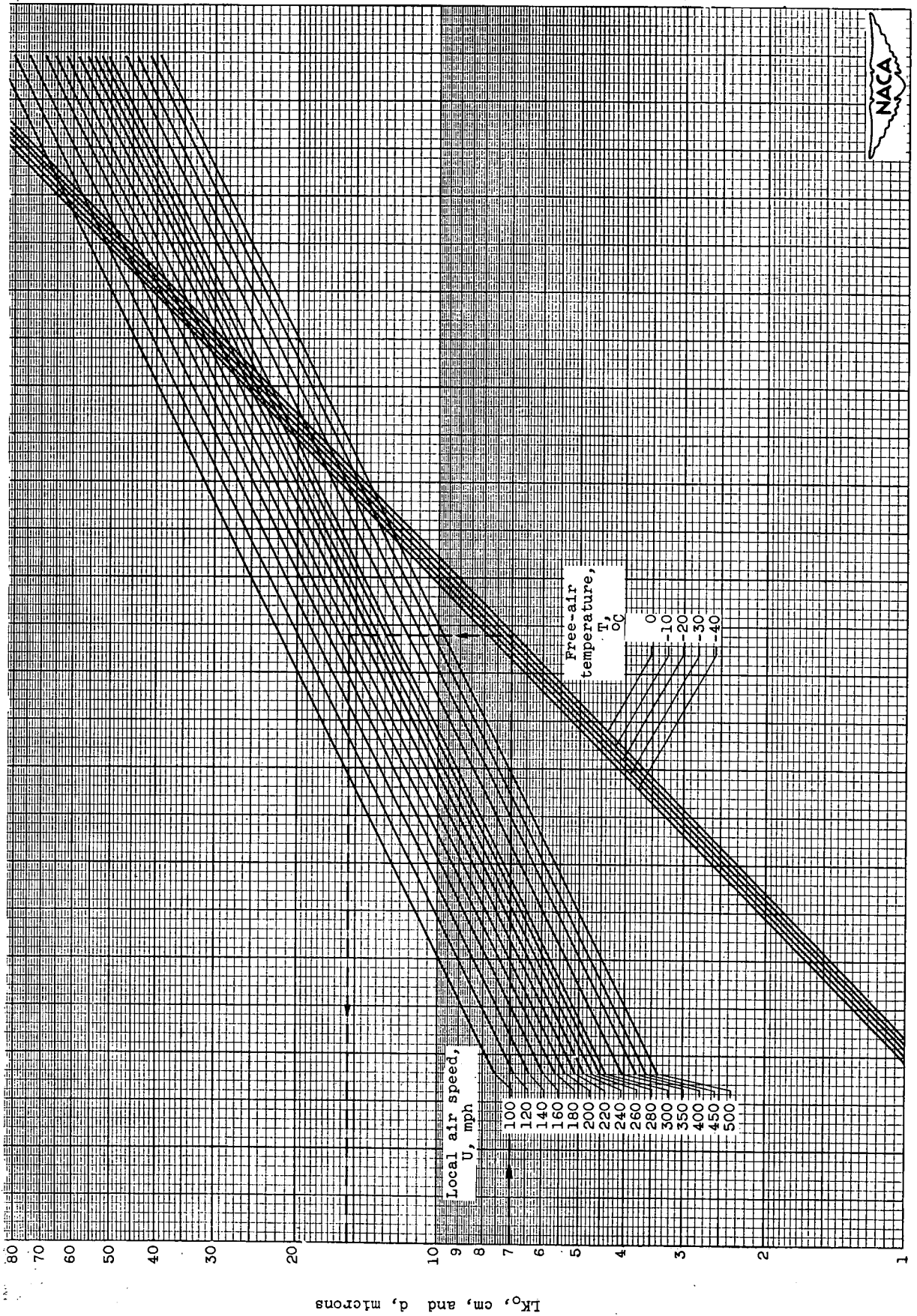
Figure 9. - Diagram for determining droplet diameter d from LK_0, free-air temperature T, and local air speed U. Enter diagram with LK_0 on ordinate, follow horizontal line to diagonal line representing temperature, follow vertical line to diagonal line representing air speed, and follow horizontal line to value of droplet diameter on ordinate. Example: $LK_0 = 7$ centimeters, T = 0° C.
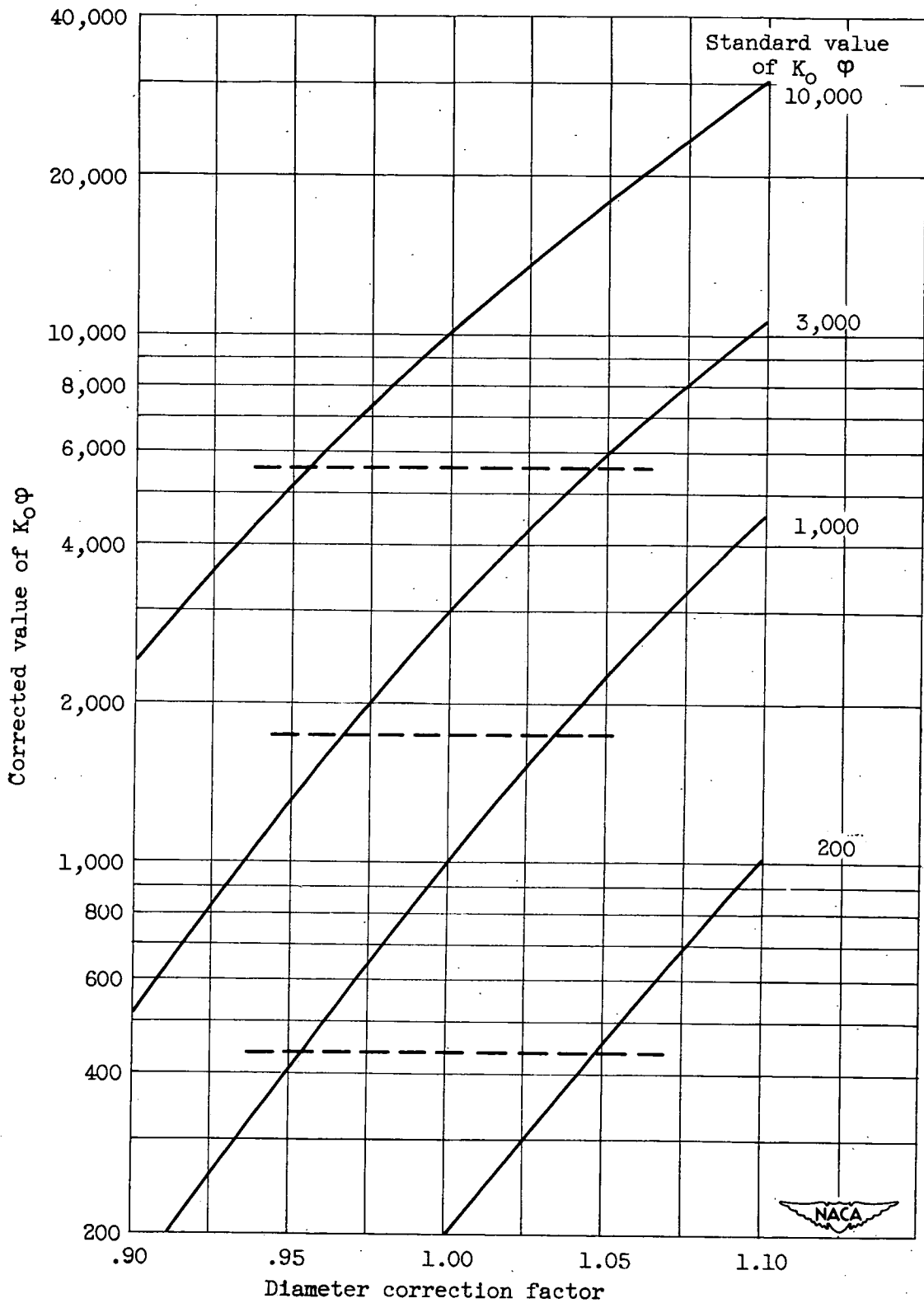
Figure 10. - Droplet-diameter correction factor.
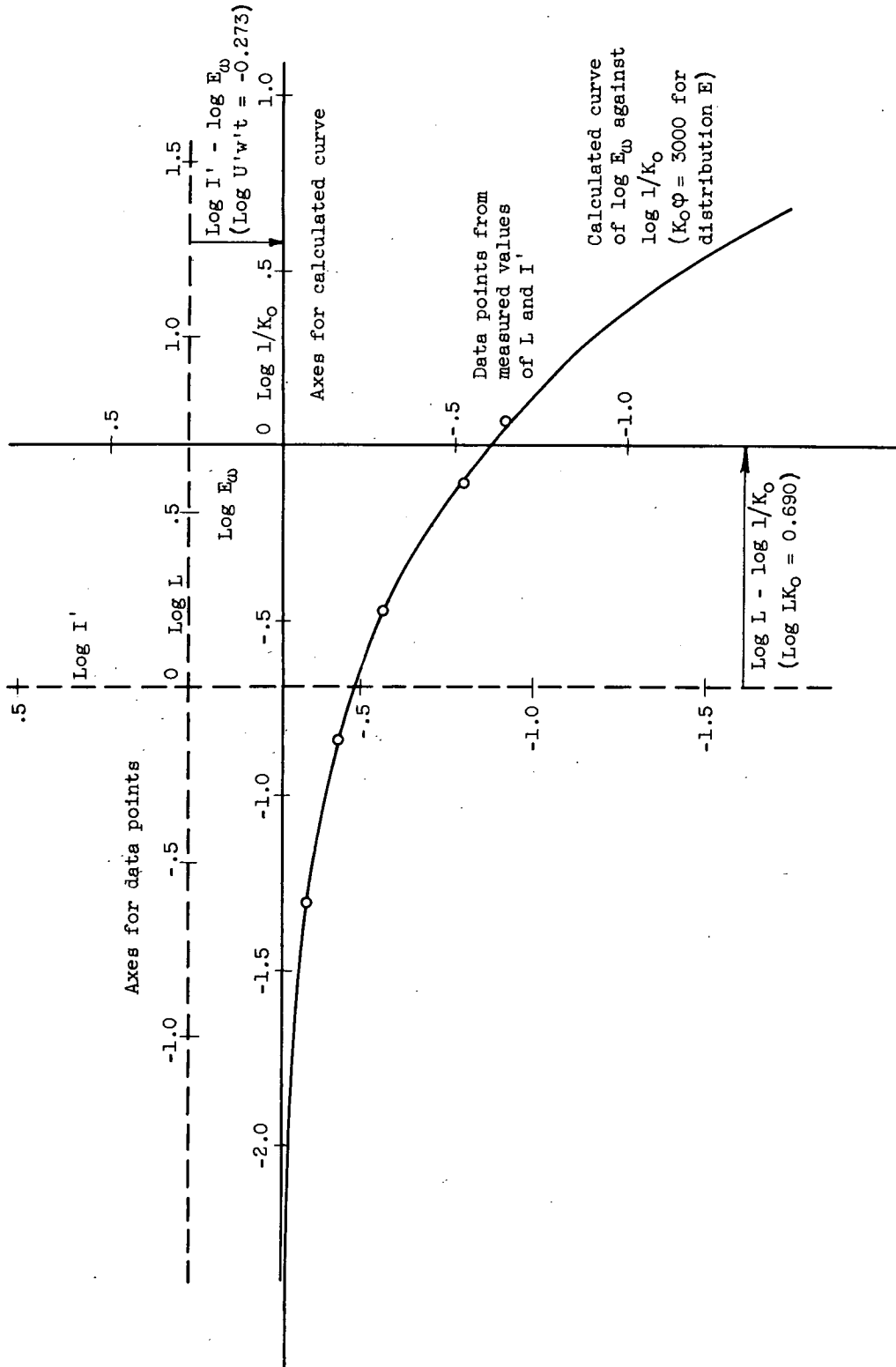
Figure 11. - Comparison of measured ice-collection data with calculated collection-efficiency curve.
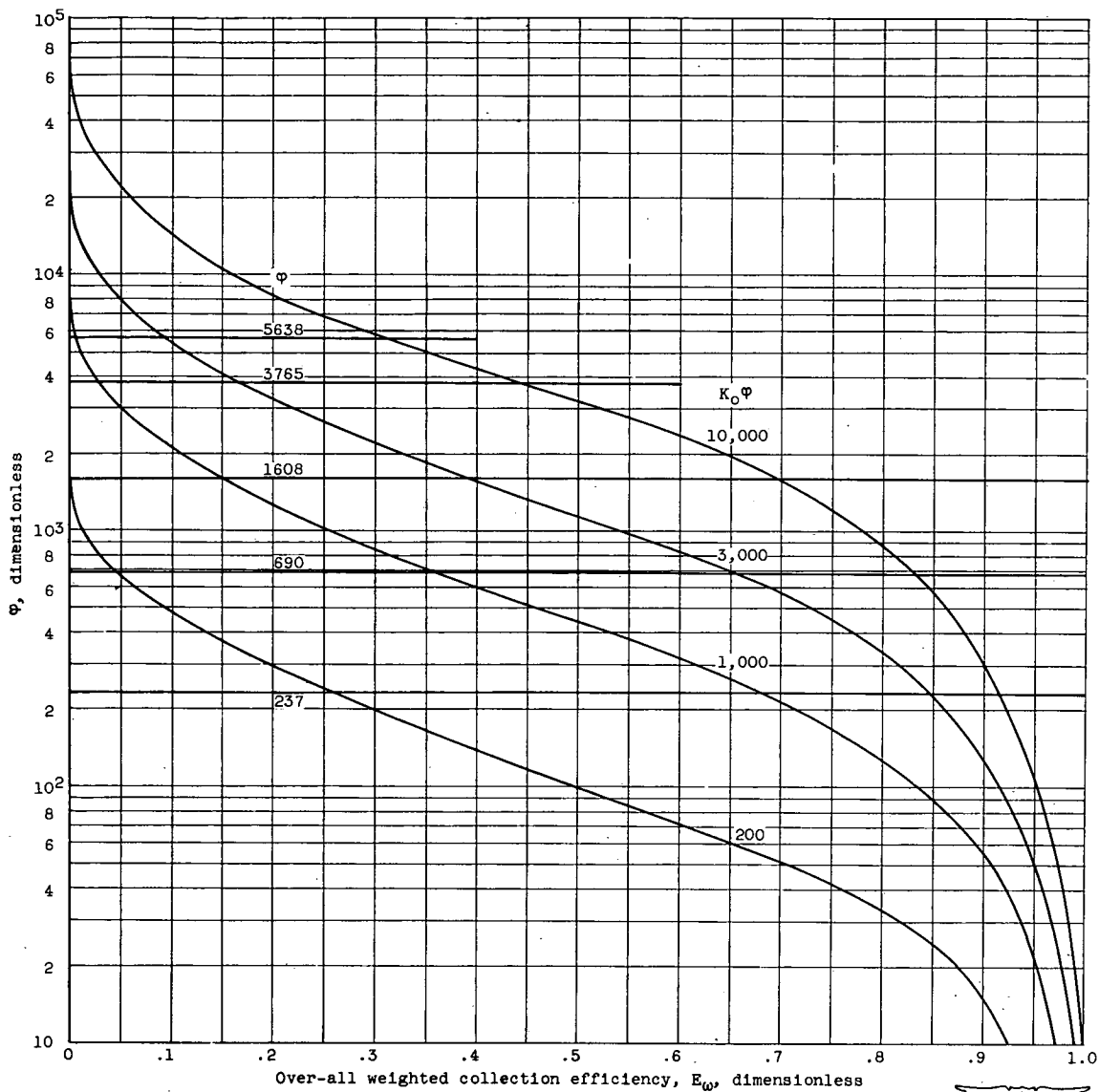
(a) Distribution A.

Figure 12. - Over-all weighted collection efficiency plotted against φ for four values of $K_0\varphi$.
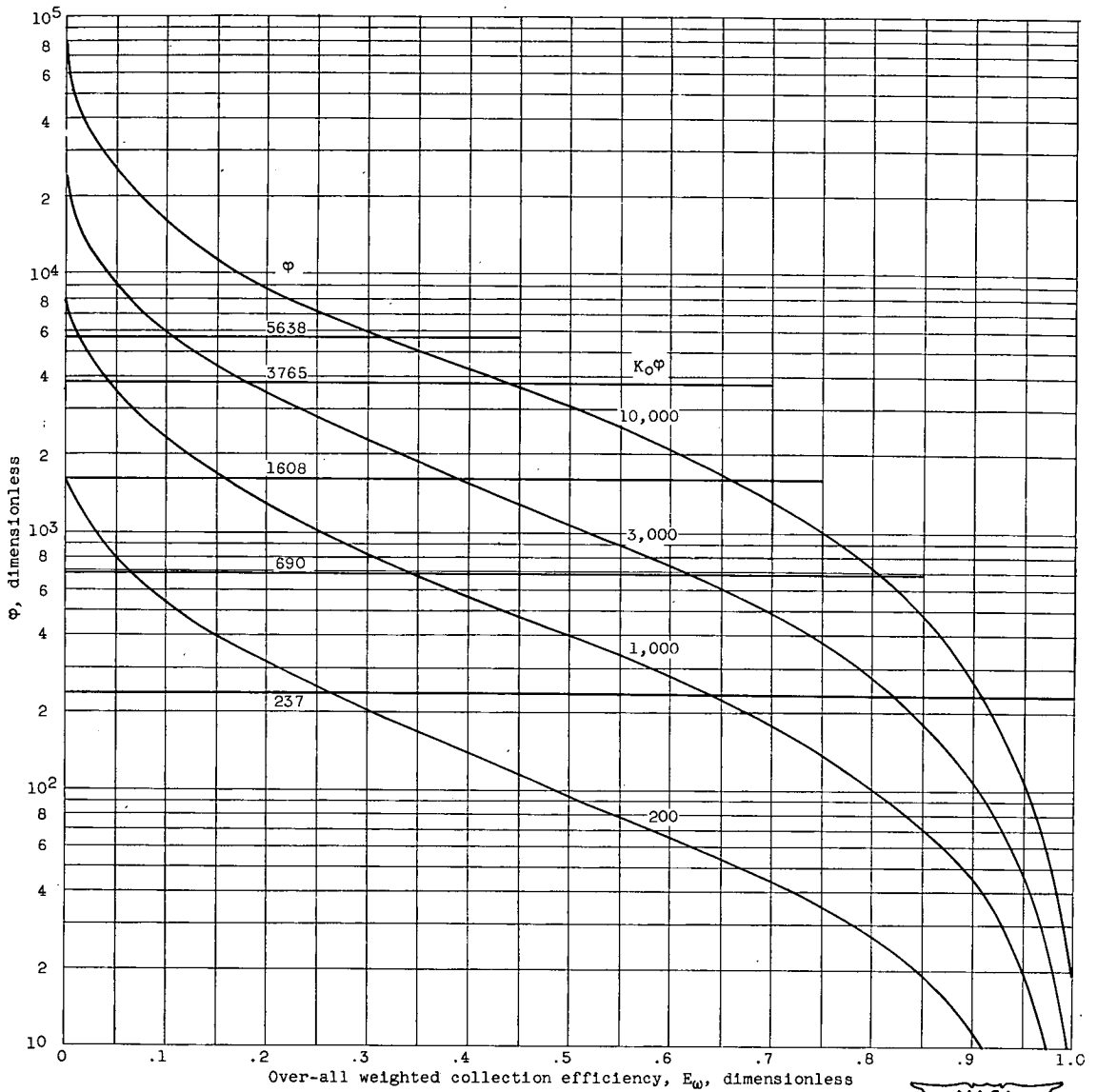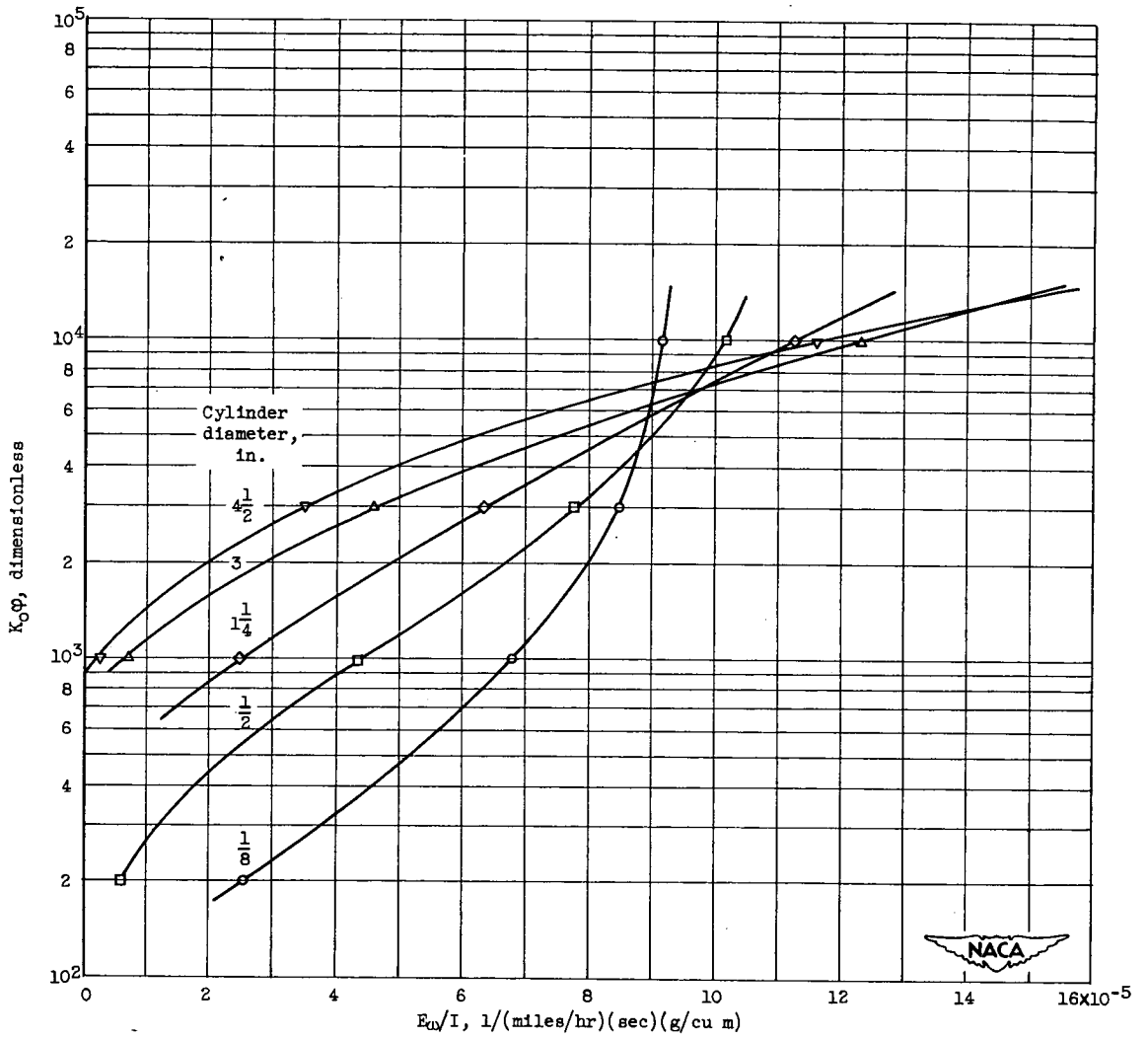
(b) Distribution C.

Figure 12. - Continued. Over-all weighted collection efficiency plotted against φ for four values of $K_0\varphi$.
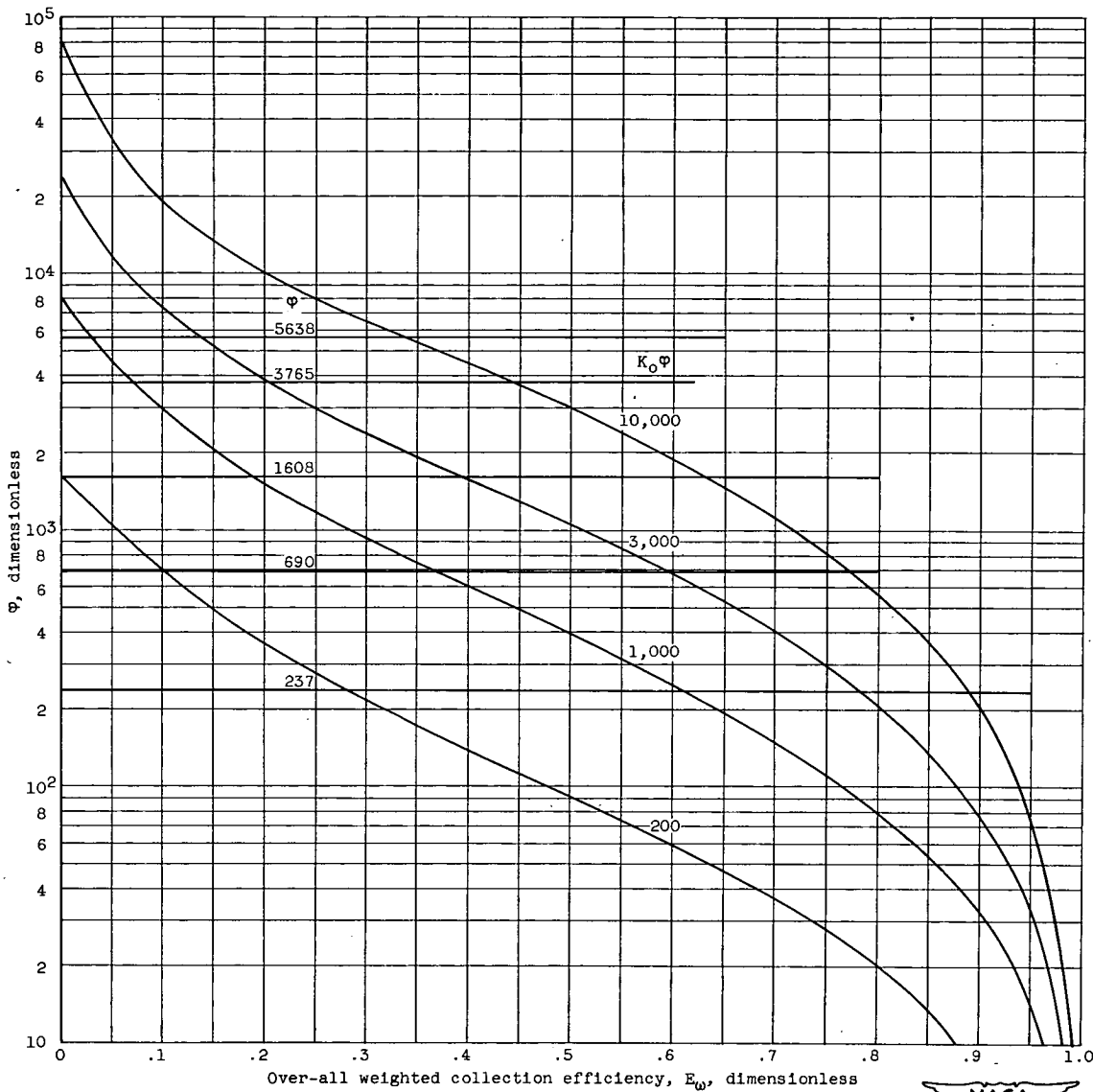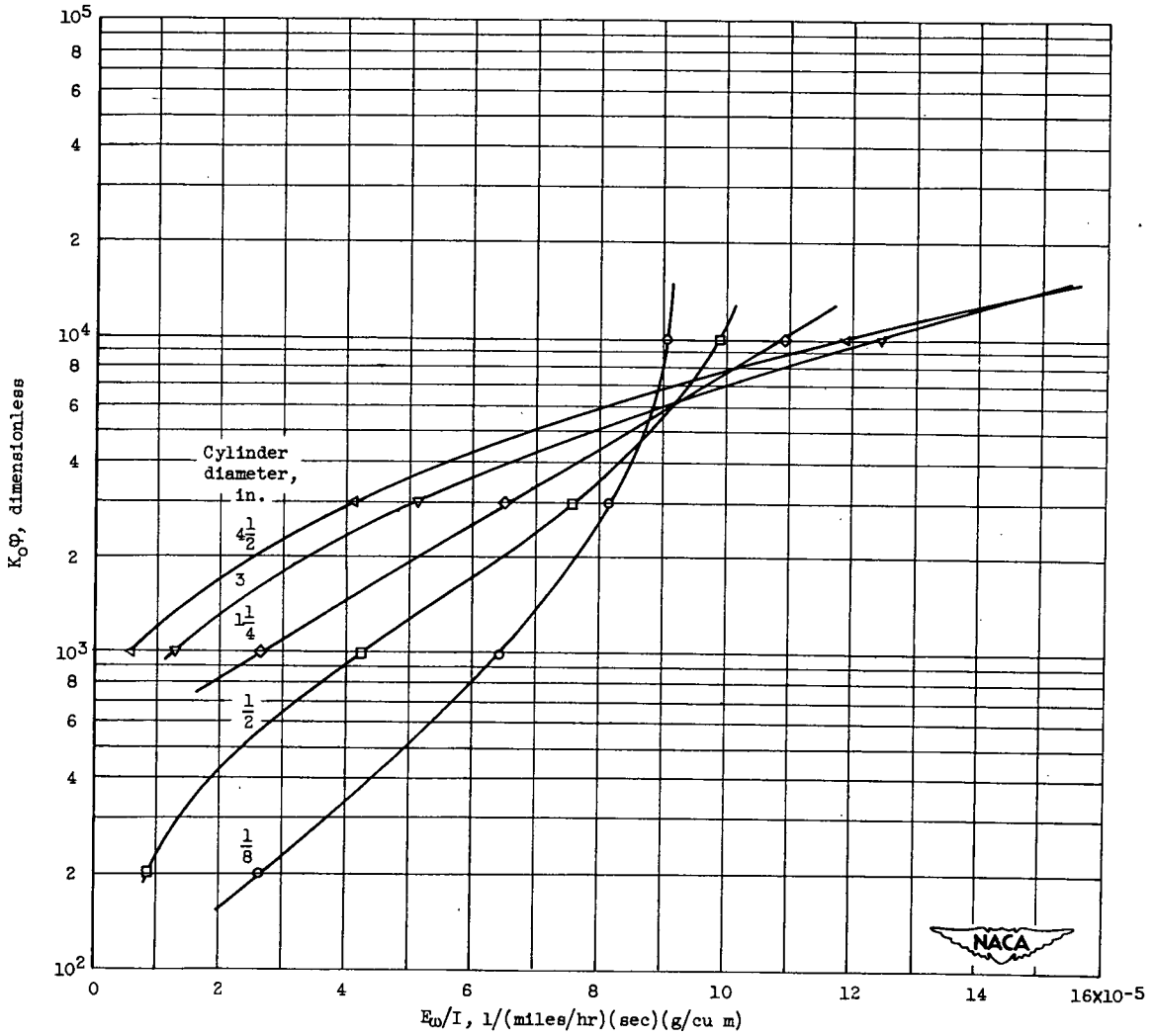
(c) Distribution E.

Figure 12. - Concluded. Over-all weighted collection efficiency plotted against φ for four values of $K_o\varphi$.
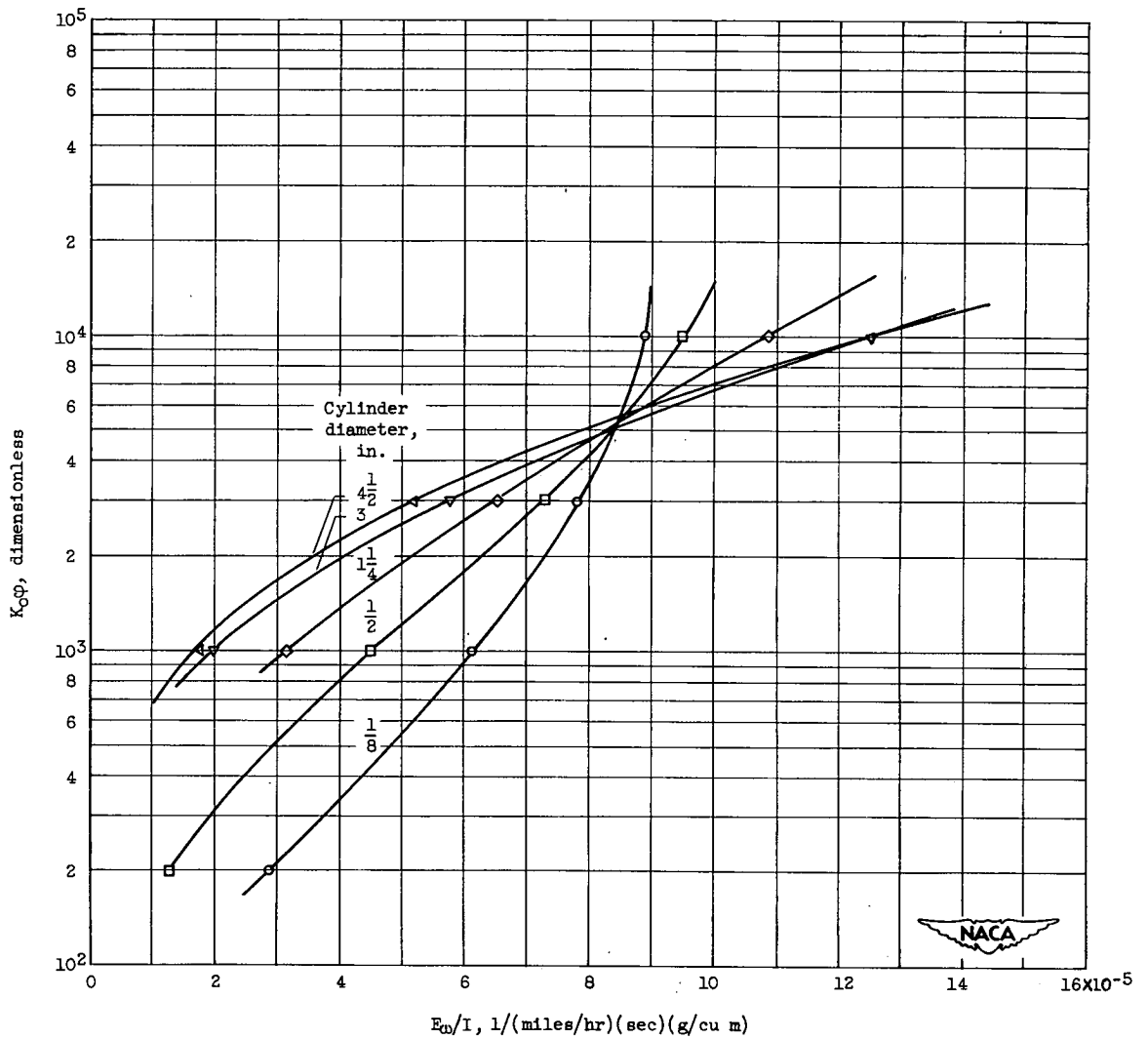
(a) Distribution A.

Figure 13. - Parameter $K_O\varphi$ as function of E_{ω}/I for various cylinder diameters.

(b) Distribution C.

Figure 13. - Continued. Parameter $K_0\varphi$ as function of E_ω/I for various cylinder diameters.

(c) Distribution E.

Figure 13. - Concluded. Parameter $K_0\varphi$ as function of E_ω/I for various cylinder diameters.